PHOTONICS Research

Silicon photonic devices for scalable quantum information applications

Lantian Feng,[1,2,3] Ming Zhang,[4] Jianwei Wang,[5,6] Xiaoqi Zhou,[7] Xiaogang Qiang,[8] Guangcan Guo,[1,2,3] and Xifeng Ren[1,2,3,*]

[1]CAS Key Laboratory of Quantum Information, University of Science and Technology of China, Hefei 230026, China
[2]CAS Center for Excellence in Quantum Information and Quantum Physics, University of Science and Technology of China, Hefei 230026, China
[3]Hefei National Laboratory, University of Science and Technology of China, Hefei 230088, China
[4]State Key Laboratory for Modern Optical Instrumentation, Centre for Optical and Electromagnetic Research, Zhejiang Provincial Key Laboratory for Sensing Technologies, Zhejiang University, Zijingang Campus, Hangzhou 310058, China
[5]State Key Laboratory for Mesoscopic Physics, School of Physics, Peking University, Beijing 100871, China
[6]Frontiers Science Center for Nano-optoelectronics, Collaborative Innovation Center of Quantum Matter, Peking University, Bejing 100871, China
[7]School of Physics and State Key Laboratory of Optoelectronic Materials and Technologies, Sun Yat-sen University, Guangzhou 510000, China
[8]National Innovation Institute of Defense Technology, AMS, Beijing 100071, China
*Corresponding author: renxf@ustc.edu.cn

Received 31 May 2022; revised 2 August 2022; accepted 3 August 2022; posted 9 August 2022 (Doc. ID 464808); published 14 September 2022

With high integration density and excellent optical properties, silicon photonics is becoming a promising platform for complete integration and large-scale optical quantum information processing. Scalable quantum information applications need photon generation and detection to be integrated on the same chip, and we have seen that various devices on the silicon photonic chip have been developed for this goal. This paper reviews the relevant research results and state-of-the-art technologies on the silicon photonic chip for scalable quantum applications. Despite the shortcomings, the properties of some components have already met the requirements for further expansion. Furthermore, we point out the challenges ahead and future research directions for on-chip scalable quantum information applications. © 2022 Chinese Laser Press

https://doi.org/10.1364/PRJ.464808

1. INTRODUCTION

Quantum information science is a new frontier subject combining quantum mechanics and information science. The quantum nature of particle superposition, entanglement, and measurement is applicable for more efficient information processing, computation, transmission, and storage. The development of quantum information industry promises more powerful computing power, high security information communications, and a deeper understanding of nature. It is expected to resolve numerous scientific problems that are difficult to be effectively solved by existing classical techniques. For example, absolutely secure information transmission [1,2], exponentially or polynomially accelerating the resolving of hard scientific problems [3,4], efficient simulation of molecular structures [5], and precision measurement beyond the standard quantum limit [6].

In the last decades, quantum fundamental science was rapidly transformed into quantum technologies with huge resources invested by global academia, research centers, and industry. Quantum scientific research is moving from the stage of principle verification of quantum rules to the stage of practical device research and development governed by these rules. We have seen the quantum computational advantage realized in different systems [7–9], quantum key distribution via thousands of kilometer-level satellite-to-ground quantum networks [10], and quantum-enhanced sensing for gravitational waves [11], magnetic fields [12], and the mass of nanoparticles [13].

Photon, as one ideal information carrier, has been widely used in quantum information processing and shows several unique advantages, such as fast transmission speed, low noise, multiple degrees of freedom for information encoding and high capacity. Besides, light has a wide range of applications in energy, communications, computation, and medical care. These increasingly mature industrial applications provide favorable supports for photonic quantum technologies. Currently, fiber optical communications technology has become the pillar for information transmission, and photonic integration and optoelectronic integration for information processing have developed rapidly in recent years for the future all-optical network. Therefore, optical quantum systems are becoming a promising platform for quantum information processing [14–16].

To enhance the complexity of quantum optical experiments, optical quantum systems tend to use integrated photonic circuits [17]. Compared to systems that use discrete optical components on an optical table, the integrated photonic

devices enable localization and manipulation of photons at micro/nano scales, thus greatly improving the stability and scalability of quantum optical experiments and providing a complex, compact quantum photonics approach for quantum communications, sensing, and computing applications [18]. Therefore, these integrated techniques will take quantum applications out of the laboratory and into large-scale and practical applications. Multiple optical waveguide materials, such as silica [19–22], silicon (Si) [23], silicon nitride (SiN) [24–27], lithium niobate [28–30], and techniques such as lithography [31] and laser writing [32] have been developed. Among those materials, silicon photonics is a good candidate because of its easy preparation, high integration density, and excellent optical properties [33]. Thanks to the leadership of classical silicon photonics in large-scale photonic integrated circuits, the performance of silicon-based devices also has been rapidly improved [34].

Currently, photonic devices on silicon chips for various quantum applications have been developed, such as high-efficiency chip-fiber couplers [35], large-scale programmable quantum photonic circuits [36], and single-photon detectors [37]. However, scalable quantum applications put forward new and greater requirements for integrated photonic devices. For example, a high-isolation, on-chip filter is needed to separate the pump and single-photon-level signals, and a modulator should also be able to operate under cryogenic conditions. In this paper, we review the relevant research results and state-of-the-art technologies related to silicon photonic chips for scalable quantum applications. Since silicon optical chips can be easily prepared, their applications are very wide and diverse. Here, we just review common CMOS-compatible silicon-on-insulator (SOI) chips with a telecom optical band O + C. Thankfully, the properties of some integrated components have already met the requirements for further quantum applications and expansion. Furthermore, we point out the challenges ahead and future research directions. This review mainly focuses on the advances related to silicon photonic devices. For more information about related quantum experiments, we recommend some related good reviews, such as the preparation of photon-pair sources with silicon photonics [38,39], advances in quantum experiments on the silicon chip [17,40], and hybrid integrated techniques for quantum applications [41,42].

This paper has a total of four sections. Section 2 reviews the state-of-the-art technologies of basic components on the silicon chip, such as on-chip photon sources, detectors, and chip interconnects. In Section 3, we introduce some key fundamental quantum information processing in silicon photonic circuits and review the research on multiphoton and high-dimensional applications, quantum error correction, quantum key distribution as well as quantum state teleportation between chips. These excellent works lead to scalable quantum computing and communications. Finally, in Section 4, we look at the future of silicon photonics for scalable quantum information applications and provide challenges for further scaling.

2. SCALABLE TECHNIQUES FOR SILICON PHOTONIC CHIPS

Scalable quantum information processing must improve the complexity of a single chip as much as possible. Different degrees of freedom of photons should achieve universal quantum operation, and the quantum photonic source, detector, logic operation and other core functions should be improved to high quality and be integrated on the same chip. Considering the limited chip size and difficulty of hybrid integration with different materials, a multifunction chip can also be achieved by high-efficiency optical interconnection for quantum communications and distributed quantum computing and metrology. Accordingly, we divide the state-of-the-art techniques in silicon photonics into two aspects to review: single-chip and interconnection technologies. This section includes single-photon sources, photon detection, wavelength and mode division multiplexing, and cryogenic techniques on a single chip and chip interconnection techniques.

A. Single-Photon Sources

Scalable quantum photonic information processing requires multiple high-quality single photon sources. Today, there are two promising approaches to achieve a near-deterministic single photon source: one is based on multiplexing an array of probabilistic parametric photon pair sources, and the other is based on solid-state single-photon emitters.

With a strong third-order nonlinear response, silicon waveguides can be directly used to prepare photon pair sources via a spontaneous four-wave mixing process (SFWM) [43]. Many techniques were developed to improve the photonic source quality, such as using microring resonators [44–46] and introducing special phase-matching conditions [47]. More details are given in Table 1. After pair generation, one of the photons is detected to herald the presence of its partner. Although each photon pair source is probabilistic, multiple heralded single photons can be dynamically switched to one single output mode, thus increasing the output probability. Any degree of freedom of the photon pairs can be used for multiplexing, such as path, frequency, and time bins. These also can be combined to multiplicatively increase the number of multiplexed modes. In Ref. [52], a 63.1% efficiency increase in the heralded single-photon output has been demonstrated through multiplexing photons generated in two silicon waveguides. In Ref. [53], the enhancement was increased to 90% $\pm$ 5% by using a silicon waveguide pumped by time and wavelength division multiplexed pulses. In Ref. [54], a 100% enhancement was achieved by multiplexing photons from four temporal modes. Recently, although not within silicon photonics, a 9.7 times enhancement in efficiency has been realized using an optical delay to multiplex 40 heralded single-photon sources [55]. Despite these developments, on-chip integration of multiplexing systems is still an outstanding challenge, and the main obstacle is the device loss. Assuming, for example, that 1 ns delay line corresponds to a 10 cm long silicon waveguide, and the waveguide has a state-of-the-art low loss of 0.08 dB/m [56], 100 ns delay line will introduce 0.8 dB loss, which is still much higher than that in commercial fiber. The integrated high-speed switch, one necessary component in multiplexing systems, usually needs ion doping or hybrid integration with other electro-optic materials such as lithium niobate [57], and these post-processing processes always introduce extra losses. A significant reduction in these losses will enable multiple near-deterministic

Table 1. State-of-the-Art Photonic Sources at Telecommunications Wavelengths[a]

Reference	Structure	Bandwidth	PGR/SER	CAR	$g^2(0)$	Wavelength
[43]	Single-mode waveguide	100 GHz	$0.7\ \mathrm{MHz}\cdot\mathrm{mW}^{-2}$	80	–	1538.2 and 1562.2 nm
[44]	Microring resonator	2.1 GHz	$149\ \mathrm{MHz}\cdot\mathrm{mW}^{-2}$	12,105	0.00533	1535.5 and 1574.7 nm
[47][b]	Multimode waveguide	4 nm	$18.6\ \mathrm{MHz}\cdot\mathrm{mW}^{-2}$	–	0.053	1516 and 1588 nm
[48]	GaN defect	3–50 nm	1.5 MHz	–	0.05	1085–1340 nm
[49][b]	2D $MoTe_2$	8.5–37 nm	–	–	0.058	1080–1550 nm
[50]	G center	0.5 nm	99 kHz	–	0.07	1278 nm
[51]	T center	255 MHz	–	–	0.2	1326 nm

[a]For heralded single-photon sources, pump power normalized pair generation rates are given. For solid-state emitters, saturated emission rates are given. PGR, pair generation rate; SER, saturated emission rate; and CAR, coincidence-to-accident ratio.

[b]Indicate the use of pulsed laser pump.

single photon sources achieved on the silicon chip with probabilistic nonlinear parametric processes.

In another approach, the solid-state emitters generate deterministic single photons and can be integrated or transferred on the silicon photonic circuits. Since silicon is opaque below around 1100 nm, single-photon emitters integrated with silicon must radiate photons beyond this wavelength limit. Multiple quantum dots at telecommunications wavelengths have been demonstrated [48,49,58–63]. Among them, the most common are semiconductor quantum dots including InAsP [58], InAs/InP [59,60], and InAs/GaAs [61,62]. By using emission-wavelength-optimized waveguides, Ref. [58] demonstrated photon emission from single InAsP quantum dot with a large tuning range from 880 to 1550 nm. With hybrid integration techniques, a transfer of semiconductor quantum dots on silicon waveguides, as shown in Figs. 1(a) and 1(a), has been implemented with $g^2(0)$ values around 0.3 [59,61,62]. By using localized defects in the gallium nitride crystal, high-quality solid-state quantum emitters in the telecom range have been achieved [48]. Even at room temperatures, $g^2(0) = 0.05$ was obtained with CW laser excitation. 2D materials show many amazing properties and have also been used to produce quantum emitters; for example, telecom-wavelength single-photon emitters via coupling 2D molybdenum ditelluride ($MoTe_2$) to nanopillar arrays have been reported with $g^2(0) = 0.058$ and $g^2(0) = 0.181$ under, respectively, pulsed and CW laser excitation [49]. Color centers, known as G centers and T centers, which originate from carbon-related defects in silicon, are becoming another kind of candidates with telecom-O band radiation [50,51,63,66]. Different from other methods, color centers can be directly integrated into silicon waveguides without hybrid integration for large-scale quantum photonic information applications [64,65]. For example, tens of thousands of individually addressed photon-spin qubits have been demonstrated with T centers, which will provide photonic links between spin qubits and greatly advance quantum information networks [51].

To integrate solid-state emitters with photonic waveguides, many approaches are proposed, such as nanoscale positioning approaches [67]. For the important coupling efficiency, Ref. [61] showed a total single-photon coupling efficiency of 63% experimentally and, in theory, higher than 99%. In Ref. [65], emitters were directly integrated into silicon waveguides and showed a 40% coupling efficiency in a simulation. In addition, the use of optical microcavities deserves further consideration to improve the extraction efficiency [68–70]. To further scale up, the simultaneous operation of multiple emitters is necessary. However, no two solid-state quantum emitters are alike when being experimentally produced. To keep coherence among them, wavelength tunability is neces-

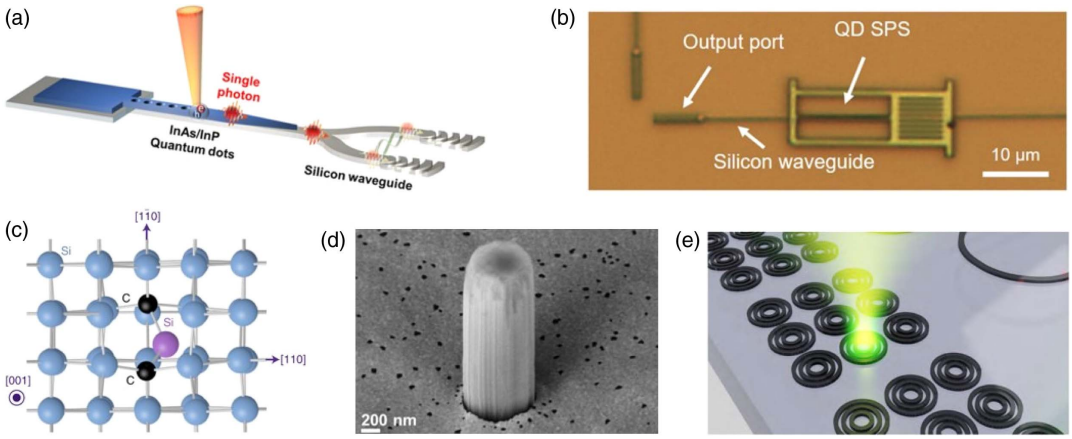

Fig. 1. Solid-state quantum emitters in silicon photonics. (a) Position grown InAs/InP quantum dots on a silicon photonic chip by the pick-and-place technique. Adapted from [59]. (b) Integrate heterogeneous optical components with a transfer-printing-based approach. Adapted from [62]. (c) Atomic structure of the G-center. Adapted from [63]. (d) Si nanopillar including the G-center. Adapted from [64]. (e) Bullseye structures used to enhance vertical coupling of G-centers. Adapted from [65].

sary. Electronic integration or induced strain has been used to tune the wavelength, and quantum interference between photons generated from independent quantum emitters has been demonstrated [71,72]. In nanophotonic devices, wavelength tuning of the selected integrated quantum emitter has been realized [73–75]. The rapid development of processing and tuning techniques has enhanced the indistinguishability of photons between different emitters and increased the number of emitters on a chip. Although not in the telecom band, quantum interference of photons from two remote quantum dots with a visibility of 93.0% [76] and large-scale integration of artificial atoms in hybrid AlN photonic circuits [77] have been recently demonstrated.

B. Photon Detection

Photon detector converts optical signals into electrical signals and is an essential part for photonic quantum information applications. For squeezed light measurement, germanium (Ge) photodetectors integrated on silicon were developed [78] and homodyne detectors have been realized based on them [79]. Furthermore, by interfacing silicon photonics with integrated amplification electronics, complete integrated homodyne detectors have been demonstrated [80] and a shot-noise-limited bandwidth of more than 20 GHz has been achieved [81].

For single-photon-level detection, superconducting nanowire single-photon detectors (SNSPDs) show excellent performance, such as near-unity system detection efficiency [82], GHz maximum count rate [37], and picosecond-level temporal resolution [83]. SNSPD uses a superconducting material that works below its critical temperature. Even if only one photon hits, the energy is enough to excite the material, and subsequently generate voltage pulses. A range of superconducting materials have been developed, including NbN [37], NbTiN [84], MoSi [85], and WSi [86]. In vertical optical coupling between fibers and SNSPDs, fiber end faces are parallel to the SNSPDs' photonsensitive surfaces, and photons are vertically incident to the nanowires. By optimizing the device's vertical optical stack design, as well as the coupling of the guided fiber mode to the active detection area of the device, a 98% system detection efficiency has been achieved [82]. For coupling between waveguides and SNSPDs, a traveling wave coupling is used, as shown in Fig. 2(a), which can achieve efficient detection of photons in the optical waveguide. This hybrid integration method directly places SNSPDs into silicon photonics, thus greatly enhancing the scalability of quantum photonic integrated circuits. For example, in Ref. [37], ballistic photon transport in silicon ring resonators has been demonstrated by exploiting high temporal resolution detectors. In addition, SNSPDs are integrated with high-quality-factor microcavities to increase the coupling efficiency, as shown in Fig. 2(b) [84], and decrease the dark count rate, as shown in Figs. 2(c) and 2(d) [87,88].

Typically, single-photon detectors operate in Geiger mode; that is, the electrical signal is generated by the readout circuit indicating the detection of one photon. However, in many experiments, it is desirable to use a detector that can resolve the number of photons. By analyzing the relationship between the photon numbers and the resistance of the nanowire, multiphoton detection was achieved with one conventional SNSPD [90]. SNSPDs that can calculate the number of photons also have been created on the AlN platform by exploring the pulse shapes of the detector output, as shown in Fig. 2(e) [89].

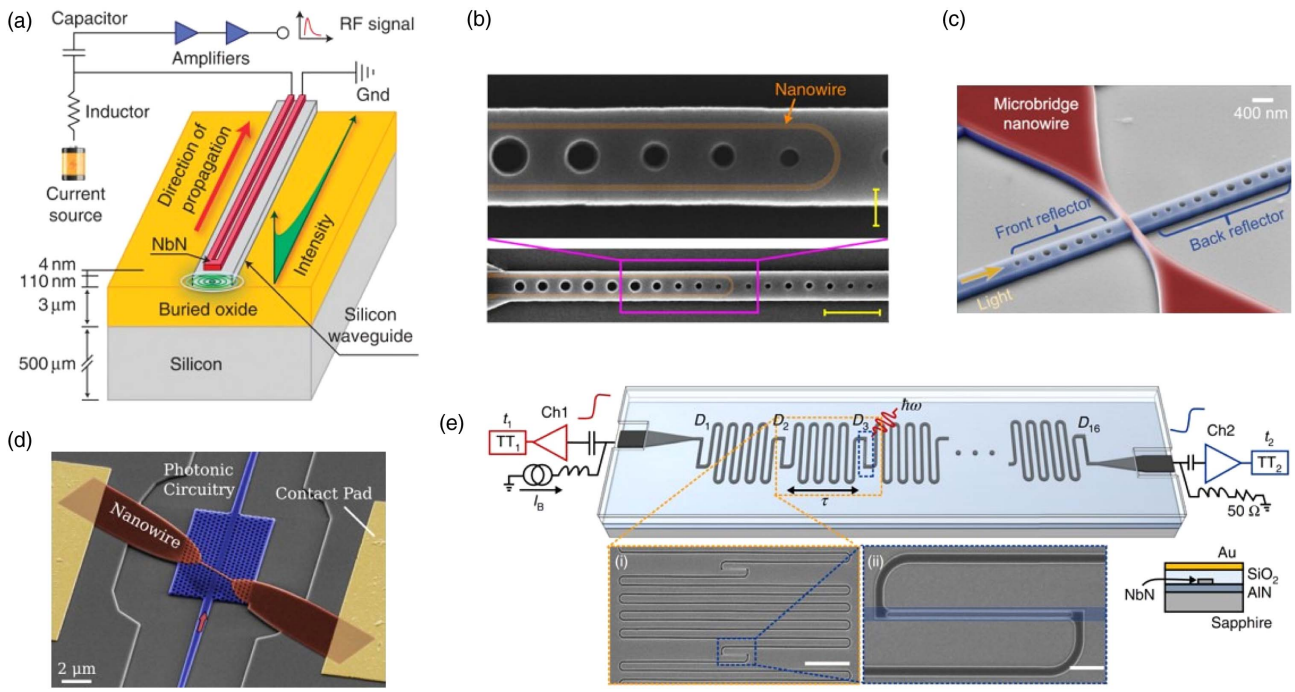

Fig. 2. Integrated SNSPDs for single-photon detection. (a) Principle of traveling wave coupling. Adapted from [37]. (b) SNSPD within a high-quality factor microcavity. Adapted from [84]. (c) Cavity-integrated SNSPD. Adapted from [87]. (d) SNSPD implemented in a two-dimensional photonic crystal cavity. Adapted from [88]. (e) A typical chain of single-photon detector segments for signal multiplexing and number resolution. Adapted from [89].

In addition, with an integrated impedance-matching taper on the superconducting nanowire, the detector's output amplitude became more sensitive to the number of photons, and a detector with photon number resolving up to four, a 16.1 ps timing jitter, and a <2 Hz dark count rate has been demonstrated [91].

The high-quality of SNSPDs boosts various novel applications, such as quantum computational advantage using photons [8], imaging and spectroscopy [92–94], and integrated quantum key distribution [95,96]. Despite the great progress achieved, SNSPDs cannot work without bulky and expensive cryogenic systems (<4 K). Other types, such as germanium-on-silicon [97,98] and InGaAs/InP single-photon detectors [99,100], are potential alternatives. For detection efficiency, germanium-on-silicon detectors have recently been demonstrated to be 38% at 1310 nm at 125 K [97], and InGaAs/InP detectors have been demonstrated to be 60.1% at 1550 nm at 300 K. A further reduction of the dark count rate will broaden their appeal in many quantum applications. More details about integrated single-photon detectors are summarized in Table 2. In addition to these conventional devices, single-photon detection based on low-dimensional materials is emerging and has shown superior performance [101].

C. Wavelength and Mode Division Multiplexing

Due to a significant increase in the demand for information processing and communications capability, much effort has been done to encode more information on one single chip. One way is to increase the integration density. Devices have been developed that are more compact and their spacing is narrower. By using the concept of symmetry breaking, for example, high-density waveguide superlattices with a low crosstalk were demonstrated [102]. This concept has also been used to construct a two-qubit quantum logic gate, and has greatly reduced the footprint [103]. Recently, an ultradense integrated multidimensional optical system with a footprint of 20 μm × 30 μm has been demonstrated based on an inversely-designed dielectric metasurface network [104]. Another way is to introduce new degrees of freedom through multiplexing, including wavelength division multiplexing (WDM) and mode division multiplexing (MDM).

WDM is a technique that encodes information with different optical wavelengths as different channels. Structures like ring resonators, unbalanced MZIs, waveguide Bragg gratings (WBGs), and arrayed waveguide gratings (AWGs) have been used in the WDM systems for wavelength multiplexing and demultiplexing [105–110]. Among them, 512 channel dense WDM [106], channel spacing down to 17 GHz [109], and hybrid integration with detectors, as shown in Fig. 3(b) [110], have been demonstrated. Although not with silicon photonics, high-speed quantum key distribution with WDM on integrated photonic circuits has been reported [113].

In addition to increasing the channel capacity, the WDM technique is also used as filters for spectrum manipulation in various optical systems [114]. With unbalanced MZIs, a programmable filter has been demonstrated and showed the tunability of the filter central wavelength, the bandwidth, and a variable passband shape [115]. With high-order ring resonators, on-chip filters are becoming ultracompact and ultrahigh-contrast, and show high flexibility [111,116–118]. Fifth-order ring resonator optical filters showed, for example, an out-of-band rejection ratio of 40 dB, and an insertion loss of only 1.8 dB within a footprint of 700 μm^2, as shown in Fig. 3(c) [116]. To increase the free spectral range (FSR), a resonator with a small radius of 0.8 μm was demonstrated and a record large FSR of 93 nm was achieved recently [118]. WBGs are FSR free and also could be employed to build filters. The add-drop structure showed high contrast and the filter bandwidths changed with the waveguide widths, as shown in Fig. 3(d) [112].

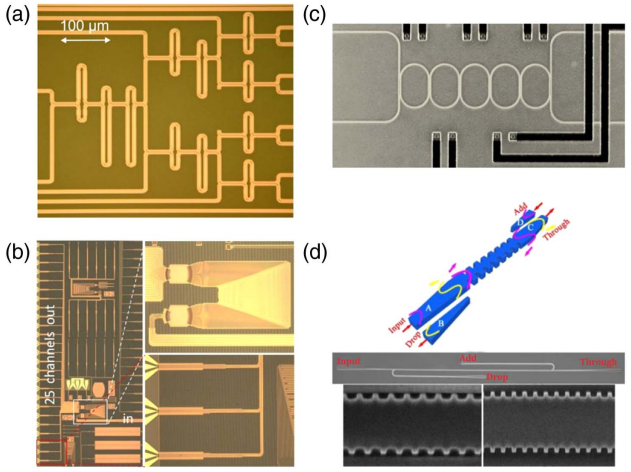

Fig. 3. Wavelength division multiplexing techniques in silicon photonics. (a) Cascaded Mach–Zehnder demultiplexer. Adapted from [105]. (b) The wavelength division multiplexing receiver chip with an integrated arrayed waveguide grating. Adapted from [110]. (c) Coupled five-ring silicon filter. Adapted from [111]. (d) Waveguide Bragg grating add-drop filter. Adapted from [112].

Table 2. State-of-the-Art Techniques for Integrated Single-Photon Detection[a]

Reference	Detection Efficiency	Jitter	Dark Count Rate	Reset Time	Temperature	Number Resolving
[37]	91%	18 ps	50 Hz	505 ps	1.7 K	–
[84]	100%	55 ps	0.1 Hz	7 ns	2.05 K	–
[87]	30%	32 ps	1 Hz	510 ps	1.7 K	–
[88]	70%	480 ps	0.1 MHz	480 ps	1.6 K	–
[91]	5.6%[b]	16.1 ps	2 Hz	85.8 ns	1.0 K	4
[98]	29.4%	134 ps	100 kHz	–	125 K	–
[100]	60.1%	–	340 kHz	88 ns	300 K	–

[a]Except in Ref. [98], whose operating wavelength is 1310 nm, all other operating wavelengths are around 1550 nm.
[b]Represent the system detection efficiency.

More details about filtering in silicon photonics are summarized in Table 3. For scalable quantum information applications, these filters will be employed to filter out the pump light before detection or separate single photons at different wavelengths, as reported in Refs. [119,120].

MDM is an emerging technique that uses the high-order transverse waveguide modes of multimode waveguides to encode more information [121]. Since multimode waveguides still support multiple wavelengths, this technique is compatible with WDM to further increase the channel capacity [122–124]. As shown in Fig. 4, various multimode silicon photonic devices have been developed for low-loss, low-crosstalk light manipulation with multiple mode channels in MDM systems, such as mode (de)multiplexers [125,130], grating couplers [131], high-speed switches [129], sharp waveguide bends, and mode-independent crossings [127,128,132]. At present, mode (de)multiplexers, including six mode channels of TE polarization and four mode channels of TM polarization, have been realized [126]. In addition, by using multimode optical waveguides with higher-order modes, some special silicon photonic devices that cannot be realized only with fundamental modes have been demonstrated, such as add-drop optical filters based on multimode Bragg gratings [112,120]. The utilization of higher-order modes for quantum photonics has stimulated many novel applications. For example, in Ref. [133], the transverse waveguide-mode degree of freedom was introduced for quantum encoding, and on-chip coherent conversion of photonic entangled quantum states among path, polarization, and transverse waveguide-mode degrees of freedom was demonstrated. In Ref. [134], quantum interference between the guided modes was demonstrated within a multimode optical waveguide. Recently, with the help of two newly developed multimode devices, a transverse mode-encoded two-qubit logic quantum gate was realized [135], and showed the potential for universal transverse mode-encoded quantum operations and large-scale multimode multi-degree of freedom quantum systems. The special intermodal phase-matching conditions were used to prepare quantum photonic sources. In particular,

Table 3. State-of-the-Art Techniques for Filtering in Silicon Photonics[a]

Reference	Structure	Size	Contrast	IL	FSR	Bandwidth
[116]	High-order microring	700 μm^2	40 dB	1.8 dB	18 nm	310 GHz (1 dB)
[111]	High-order microring	3000 μm^2	50 dB	3 dB	7.3 nm	11.6–125 GHz (3 dB)
[115]	Unbalanced MZIs	2 mm^2	15 dB	9 dB	0.8 nm	0.61, 0.34, and 0.21 nm (3 dB)
[112]	WBG	600 μm^2	35 dB	0.6 dB	–	3 nm (3 dB)
[119]	Cascaded WBG	1280 μm^2	65 dB	3 dB	–	1–2 nm (3 dB)
[120]	Cascaded WBG	3105 μm^2	60 dB	2 dB	–	5.5 nm (3 dB)

[a]MZI, Mach–Zehnder interferometer; WBG, waveguide Bragg grating; IL, insertion loss; and FSR, free spectral range.

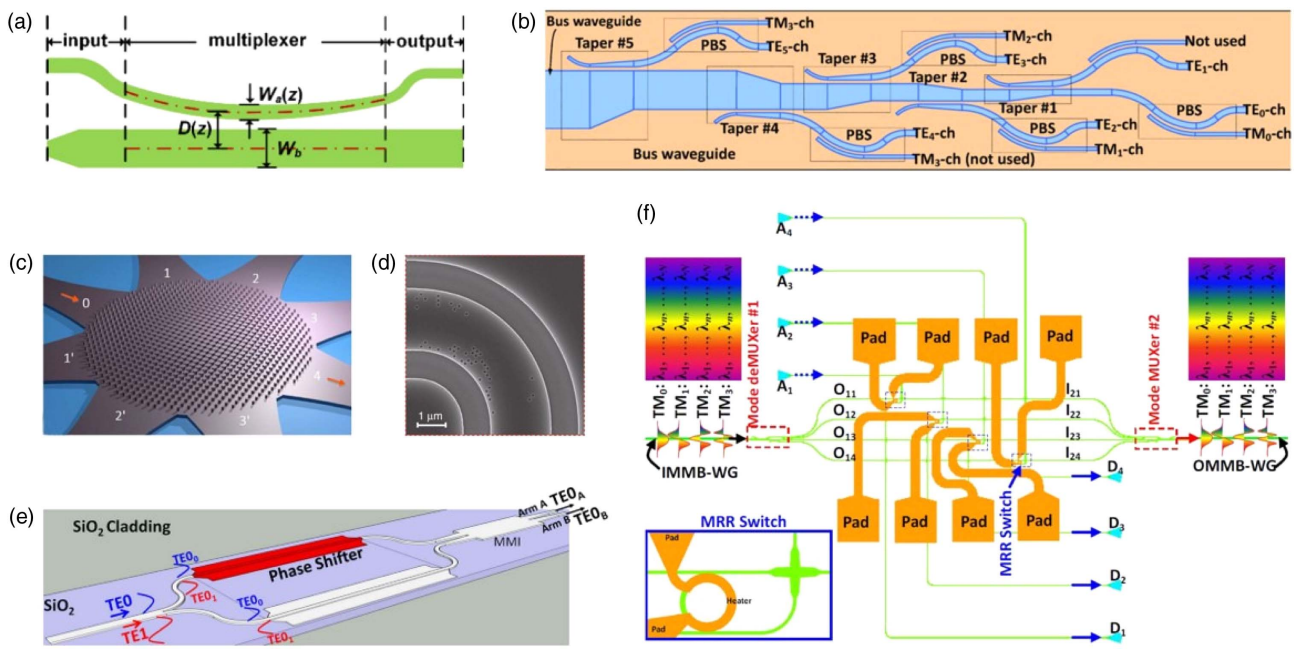

Fig. 4. Mode division multiplexing techniques in silicon photonics. (a) Mode (de)multiplexer with adiabatic taper. Adapted from [125]. (b) Mode (de)multiplexer. Adapted from [126]. (c) Multiport multimode waveguide crossing using a metamaterial-based Maxwell's fisheye lens. Adapted from [127]. (d) Digital metastructure-based multimode bending. Adapted from [128]. (e) High-speed optical two-mode switch. Adapted from [129]. (f) Reconfigurable optical add-drop multiplexer for hybrid wavelength/mode-division-multiplexing systems. Adapted from [124].

an on-chip transverse mode entangled photon pair source via SFWM in a multimode waveguide was demonstrated [136]. Furthermore, by exploiting a special excitation scheme in low-loss multimode waveguides, a quantum photonic source was engineered to high spectral purity and mutual indistinguishability through intermodal SFWM [47].

D. Cryogenic Techniques

The large-scale expansion of quantum photonic integrated circuits requires the integration of all functions on a single chip, including quantum photonic sources, state manipulation, and photon detection. Because common and efficient SNSPDs must work at cryogenic temperatures (for example, 2 K), quantum photonic sources and state manipulation processes should also extend to the same temperature conditions. In addition, in quantum networks, optical interfaces with other quantum systems such as semiconductor and superconducting quantum computing systems also must operate the whole system at cryogenic temperatures.

While passive optical components can often be used directly at low temperatures, implementation of active components and nonlinear processes has been a prominent challenge. At present, quantum state manipulation structures used in quantum photonic chips at ambient conditions are generally based on the thermo-optic effect. However, the thermo-optic coefficient of silicon decreases significantly at low temperatures [137]. In particular, when the temperature is several Kelvins, the thermo-optic coefficient is four orders of magnitude lower than that at room temperature, which makes it difficult for thermo-optic modulators to work. Another problem is that, as temperatures drop, so does the available cooling capacity of the cooling system. Therefore, modulators operating at cryogenic conditions should maintain very low power consumption and heat production.

To date, some works have been reported on cryogenic modulation [138–140] with silicon photonics. In Ref. [138], by doping at higher concentrations, one microdisk modulator, shown in Fig. 5(a), that has been prepared by the plasma dispersion effect has been achieved at temperature 4.8 K and data transmission rates up to 10 Gb/s have been achieved. As the first successful implementation, this work opens the door to use silicon photonics to interface with other systems under cryogenic conditions. In addition, electro-optic modulation achieved at temperature 4 K using the Pockels effect of integrated barium titanate ($BaTiO_3$) devices has been reported, as shown in Fig. 5(b) [139]. This material showed an effective Pockels coefficient of 200 pm $\cdot$ V^{-1} at 4 K, and the fabricated devices showed high electro-optic bandwidth (30 GHz), ultra-low power consumption, and high-speed data modulation (20 Gb/s). Another implementation employed the DC Kerr effect of the silicon waveguides and achieved phase modulation at a temperature of 5 K and GHz speeds, as shown in Fig. 5(c) [140]. Despite these progresses, these modulation devices are still in the initial research stage, and the relevant applications in quantum information research have not been demonstrated. For large-scale quantum information applications, they should be more compact and have a lower excess loss. More recently, programmable Mach–Zehnder meshes have been realized using aluminium nitride (AlN) piezo-optomechanical actuators

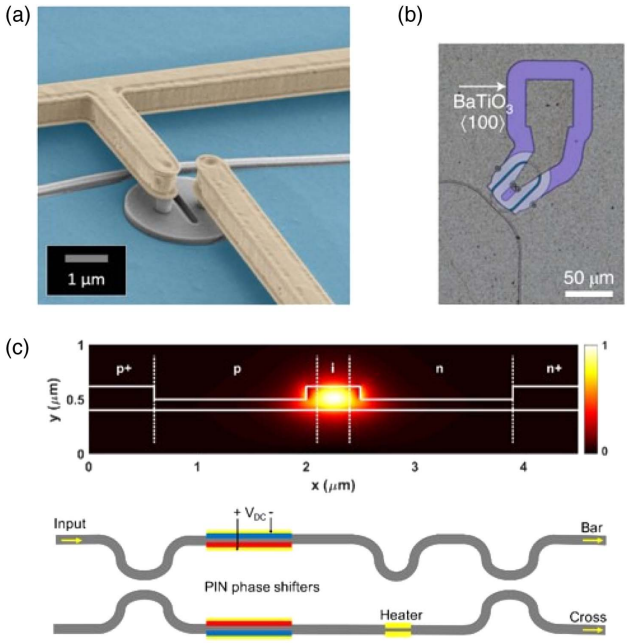

Fig. 5. Silicon photonic modulators at cryogenic temperatures. (a) The plasma dispersion microdisk modulator. Adapted from [138]. (b) The $BaTiO_3$-Si racetrack resonator. Adapted from [139]. (c) The integrated PIN junction modulator and unbalanced Mach–Zehnder interferometer composed of the modulator. Adapted from [140].

coupled to SiN waveguides [141], which can also operate under cryogenic conditions. Although the modulators operate in the visible band and on the SiN platform, the work demonstrates the possibility of on-chip, large-scale cryogenic modulation.

In addition to cryogenic modulation, some works have also been reported on cryogenic nonlinear processes in silicon photonics [142–144]. In Ref. [144], the temperature dependence of the two-photon absorption and optical Kerr nonlinearity of a silicon waveguide with temperatures from 5.5 to 300 K was measured, and the nonlinear figure of merit was found to be improved at cryogenic temperatures. Quantum applications, however, such as quantum photonic sources prepared by a cryogenic SFWM, has not yet been demonstrated.

E. Chip Interconnects

Chip interconnection plays a key role in building large-scale quantum networks. In photonic quantum technologies, chip interconnection needs efficient transfer of optical signals among different optical components. However, due to a mismatch in the effective mode sizes between different components such as fibers and silicon waveguides, special coupling structures are needed [35].

A grating coupler is one such common structure that enlarges the mode size of the waveguide by etching diffraction gratings on the waveguide surface [145]. The cross-section view of the uniform surface-corrugated grating structure is shown in Fig. 6(a), and the picture of one fabricated grating coupler is shown in Fig. 6(b). Typically, grating couplers have an alignment tolerance value of ± 2 μm for 1 dB excess losses and a more than 20 nm 1 dB bandwidth. The relaxed spatial alignment tolerance facilitates multipath alignment, which is one

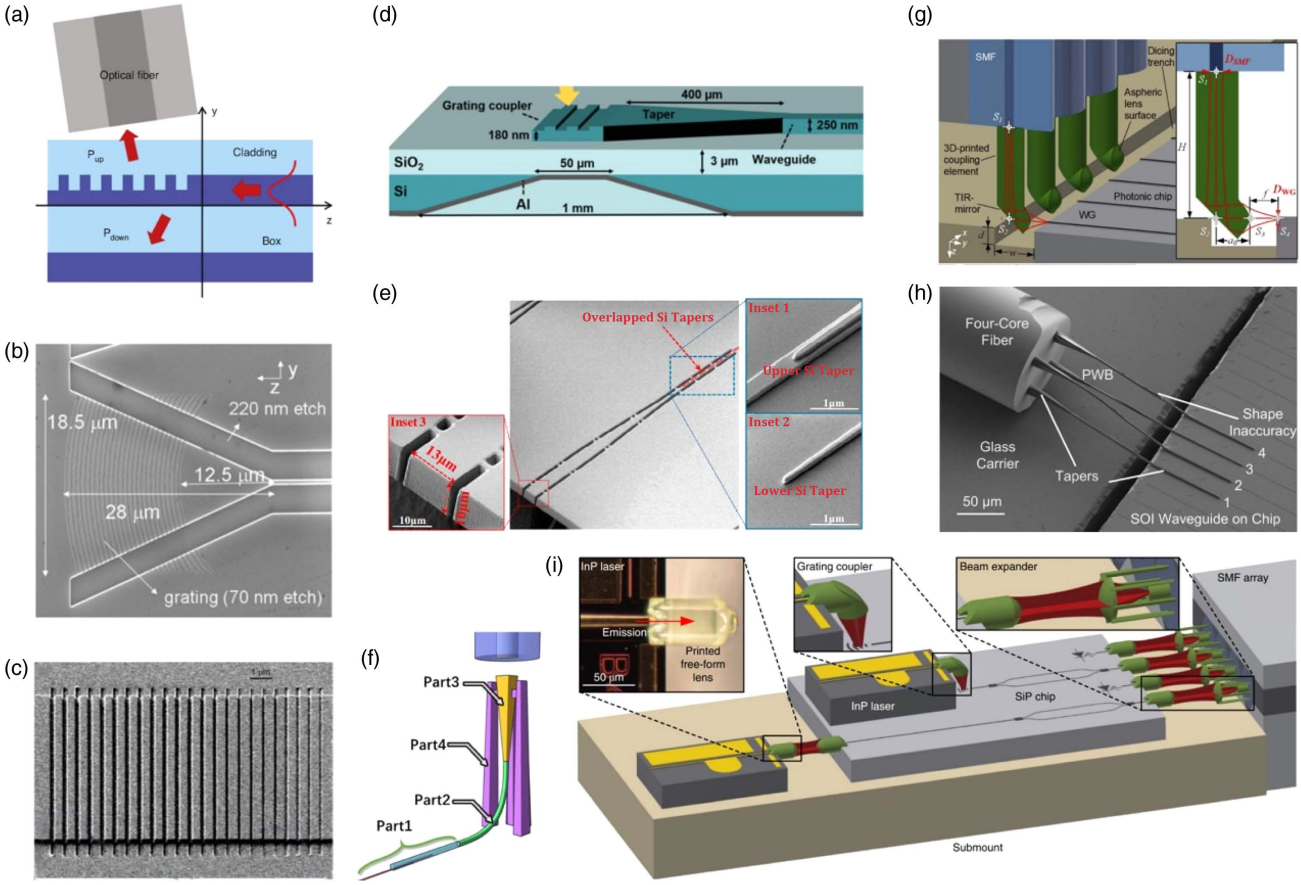

Fig. 6. Chip interconnection techniques in silicon photonics. (a) Diffraction grating-based coupling structure. Adapted from [35]. (b) The focusing grating. Adapted from [146]. (c) The double-etched apodized waveguide grating coupler. Adapted from [147]. (d) The grating coupler with a single aluminum backside mirror. Adapted from [148]. (e) The mode-size converter as end coupler. Adapted from [149]. (f) Coupler structure. Adapted from [150]. (g) The 3D-printed optical probes on the fiber end faces. Adapted from [151]. (h) Fiber cores and different silicon waveguides connected by photonic wire bonds. Adapted from [152]. (i) *In situ* 3D nanoprinted free-form lenses and expanders. Adapted from [153].

key part for scalable photonic information applications. Since quantum signals are difficult to amplify, the losses should be reduced as much as possible. For a uniform grating structure, the grating couplers have a typical coupling efficiency of 5 dB [146]. To improve the coupling efficiency, different principles and techniques have been introduced. One method is to spatially vary fill factors and etch depths, as shown in Fig. 6(c), which can achieve larger overlap integral values between the field profiles of light from the grating coupler structure and the optical fiber [147,154–157]. These apodized grating couplers have achieved a typical coupling efficiency of 1 dB. Considering that a substantial portion of the optical power input is lost in the substrate due to the diffraction downward from the grating structure, as shown in Fig. 6(a), another rule is to improve the radiation directionality. Many techniques were developed, such as using overlay grating elements [158] and substrate metal mirrors, as shown in Fig. 6(d) [148]. These techniques can especially improve both the overlap integral and directionality [159], and a below 1 dB coupling loss was achieved in this way [160]. It is worth mentioning that such high-efficiency grating couplers have been employed and played an important role in multiphoton quantum information processing on silicon photonic circuits [161–163]. The grating couplers are typically polarization dependent. To use the polarization degree of freedom to encode quantum information, 2D grating couplers are always used, which are able to couple orthogonal polarization of light into separate waveguides [164].

An end coupler is another common structure for chip–fiber coupling. Designs of the tapered waveguide have been introduced to enlarge the effective mode size of integrated silicon waveguides, as shown in Fig. 6(e). Similar to grating couplers, end couplers have also achieved below 1 dB coupling losses with commercial single-mode fibers [149,165,166]. In addition, the end couplers can achieve greater 1 dB bandwidth and support the simultaneous and efficient coupling of two polarization modes, shown in Table 4. The location on the chip edges facilitates direct packaging with the fiber array, despite requiring additional dedicated fabrication steps, such as chip dicing and polishing. Multichannel packaging with end coupling has been demonstrated for deep learning [169] and quantum transport simulations [170]. Similar to end coupling, a 3D fabricated polymer coupler showing a coupling loss of 1 dB was demonstrated recently, as shown in Fig. 6(f) [150].

In addition to fabricating complex coupling structures on a chip, many other efficient approaches are also worth considering. For example, 3D-printed optical probes on the fiber end

Table 4. State-of-the-Art Techniques for Chip Interconnection in Silicon Photonics[a]

Ref.	Technique	Loss	Bandwidth
[160]	Grating coupling	0.58 dB (TE)	71 nm (3 dB)
[165]	End coupling (tapered fiber)	0.36 dB (TM); 0.66 dB (TE)	>80 nm (1 dB)
[149]	End coupling (SMF)	2.0 dB (TM); 1.2 dB (TE)	>120 nm (1 dB)
[166]	End coupling (SMF)	1.3 dB (TM); 0.95 dB (TE)	>100 nm (1 dB)
[150]	3D vertical coupling	1 dB (TE and TM)	170 nm (TE); 104 nm (TM) (1 dB)
[151]	3D printing	1.9 dB	–
[152,167,168]	Wire bonding	0.4 dB	–
[153]	*In situ* 3D nanoprinting	0.6 dB	–

[a]For wire bonding and *in situ* 3D nanoprinting techniques, different coupling efficiencies were reported for coupling different structures. Here, the maximum values are given.

faces, as shown in Fig. 6(g), that can realize the detection of vertical cutting edge devices, were recently demonstrated with a 1.9 dB coupling loss [151]. Photonic wire bonding and *in situ* 3D nanoprinting are other novel, promising techniques for chip-scale multiplatform interconnections, as shown in Figs. 6(h) and 6(i). Using polymer waveguides with 3D geometry, photonic wire bonding can bridge photonic circuits on different chips [152,167,168,171]. With this technique, a 1.6 dB coupling loss between silicon chips [167], a 1.7 dB coupling loss between a four-core fiber and a silicon chip [152], and a 0.4 dB coupling loss between an indium phosphide chip and a silicon photonic chip [168] were demonstrated. An *in situ* 3D nanoprinting technique exploits direct-write, two-photon laser lithography to create ultracompact elements such as lenses and expanders, which can be directly integrated onto surfaces of optical integrated devices [153]. These elements can be optimized according to the coupling objectives, thus increasing the flexibility. In Ref. [153], coupling efficiencies of up to 0.6 dB between edge-emitting lasers and single-mode fibers and 2.5 dB between lasers and passive chips were achieved. Introducing these two new technologies into integrated quantum photonics will greatly improve the chip complexity and integration.

3. SCALABLE QUANTUM INFORMATION APPLICATIONS

After decades of development, silicon photonics has made a series of significant advances in quantum computing, quantum simulation, quantum communications, and metrology. Here, we give a review of some important advances in recent years. They are fundamental and have irreplaceable values in the extended applications of quantum information processing, including multiphoton and high-dimensional applications and quantum error correction on one single chip, and quantum key distribution and state teleportation among chips.

A. Multiphoton and High-Dimensional Applications

Assuming that a system contains n photons with m dimensions, the system capacity is m^n. Therefore, increasing the number of photons will improve the system capacity exponentially, and it is vitally important. Although multiple solid-state quantum emitters can be integrated on the same chip and multiple determinate single photons can be generated, controlling emitters to ensure indistinguishability between photons remains a major difficulty. Through multiplexing techniques, a single emitter can also generate multiple identical photons and complex quantum states [172,173]; however, there are still difficulties in on-chip integration of multiplexing components. As an alternative approach, SFWM can generate multiple photons directly on a single chip and relevant work in this area has made great progress in recent years.

With a strong third-order nonlinear response, silicon waveguides and microring resonators have been used to generate entangled photon pairs with different degrees of freedom [43,136,174–177] and to demonstrate various optical quantum applications [178–181]. Furthermore, multiple photon pairs were multiplexed to generate quantum states with more photons. In 2011, Ref. [182] performed a quantum interference experiment with two heralded photons generated in two independent silicon waveguides. A visibility of 73% was observed. Later, in 2018, this multiphoton interference process was demonstrated on one single chip with heralded photons from two independent microring resonator sources and an interference fringe visibility of 72% was measured [183]. Almost at the same time, silicon waveguides have been used to prepare complex four-photon states [184] and frequency-degenerate entangled four-photon states [185]. These works stimulate more multiphoton applications in integrated optical chips, such as the preparation of programmable four-photon graph states [186], the generation and sampling of quantum states of light, as shown in Fig. 7(a) [161], and the observation of nonlocal quantum interference [190]. So far, the number of photons on one single silicon chip has been increased to eight [161] and more photons could be achieved by further reducing losses. To increase the quality of multiphoton interference, different strategies have been demonstrated to improve the spectral purity of photon pairs [45–47]. In particular, Ref. [47] has achieved on-chip heralded two-photon quantum interference with a visibility of 96%, as shown in Fig. 7(b). These high-quality integrated photonic sources are promising in practical quantum applications.

High-dimensional encoding is another feasible approach to a larger system capacity. Moreover, it shows many unique quantum properties and provides improvements in particular applications such as higher capacity and noise robustness in quantum communications [191] and higher efficiency and flexibility in quantum computing [192]. On integrated chips, many degrees of freedom can be used for high-dimensional encoding, such as path, transverse-mode, frequency, and time bins. Among them, path encoding is the most common because

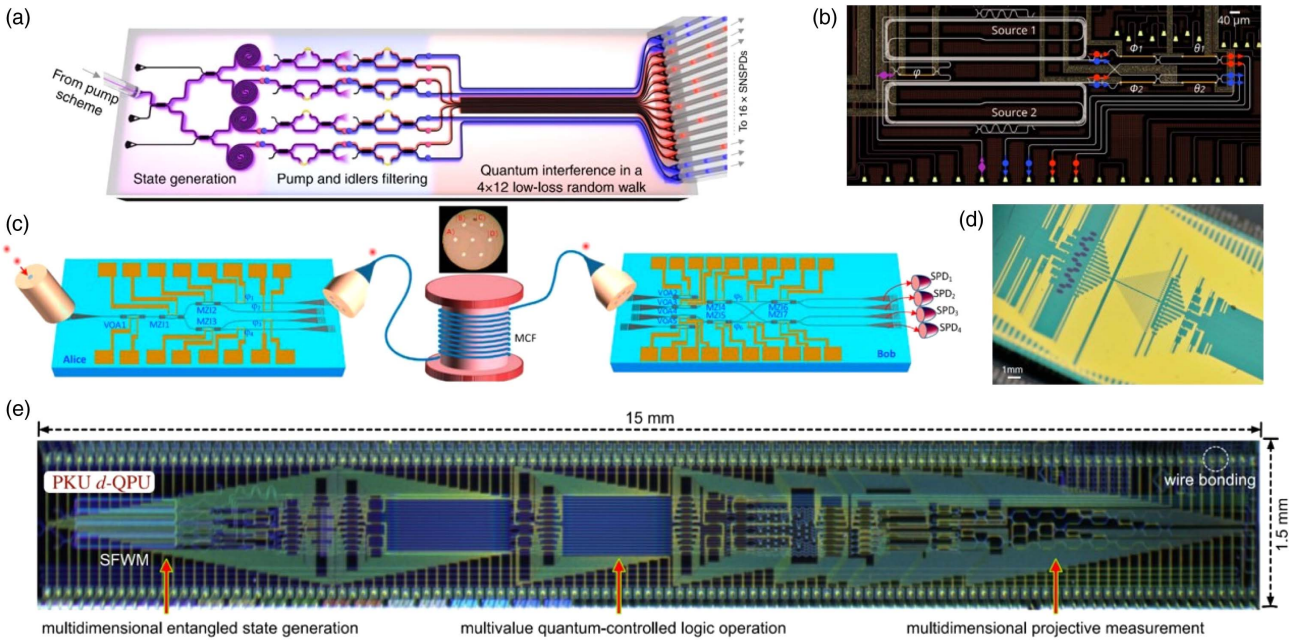

Fig. 7. Multiphoton and high-dimensional applications with silicon photonic devices. (a) Silicon photonic chip for the generation and sampling of quantum states. Adapted from [161]. (b) Coherent pumping of two sources and processing of the emitted photons. Adapted from [47]. (c) Chip-to-chip high-dimensional quantum key distribution based on multicore fiber. Adapted from [187]. (d) Silicon device for multidimensional quantum entanglement. Adapted from [188]. (e) Programmable qudit-based quantum processor. Adapted from [189].

of its ease of implementation. With an on-chip beam splitter and Mach–Zehnder interferometers, photons can be routed and manipulated in multiple paths. A coupled waveguide array also can be used to construct the desired dynamic evolution Hamiltonian for research into quantum walk, boson sampling, and quantum simulation.

For high-dimensional quantum applications with integrated devices, Ref. [187] experimentally demonstrated high-dimensional chip-to-chip quantum interconnection for the first time in 2017, as shown in Fig. 7(c). High-dimensional quantum information generated in one silicon photonic chip has been distributed to another chip through one multicore fiber. Combined with on-chip quantum photonic sources, programmable high-dimensional bipartite entangled systems have been realized [188,193]. Recently, a programmable qudit-based quantum processor including all key functions for initialization, manipulation, and measurement of two quantum quart states and multivalue quantum-controlled logic gates has been demonstrated on a silicon chip, as shown in Fig. 7(e) [189].

Despite the path, other degrees of freedom also have advantages in increasing the system capacity. For example, integrated photonic sources always have multiple frequencies [38] and the waveguide transverse-mode shows a compact way to accomplish parallel encoding [126]. Furthermore, it is effective to use multiple degrees of freedom of a quantum particle simultaneously [133]. The development of on-chip conversion devices will greatly increase the application prospects of these degrees of freedom.

B. Quantum Error Correction

Despite many natural advantages, a quantum information processor faces one basic difficulty; that is, the errors. When the product of logical operations and error rates of qubits reaches a certain level, the logical operations will lose their reliability. Meanwhile, due to the quantum no-clone theorem, qubits cannot be copied, and eliminating errors by repetition, as in classical processors, is impossible. Therefore, effective quantum error correction is a necessary step to realize one realistic quantum processor. In photonic quantum technologies, photon loss, quality of quantum states, and imperfect logical operations are all sources of errors. Various schemes were developed to improve the fault-tolerant capability with photons, such as the efforts to decrease fabrication imperfections to obtain high-performance optical components. In Ref. [194], a 60 dB extinction ratio MZI can be achieved with improved design, which equivalently can implement a single-qubit quantum gate with 99.9999% fidelity.

Another famous method is the generation of large-scale cluster states for measurement-based quantum computation (MBQC) [195–197], which depends on a sequence of local measurements on a special entangled state called the cluster or graph state. MBQC is equivalent to the circuit-based quantum computation model and, since it is relatively easy to prepare this kind of entangled state with nonlinear photonics, this model is highly valued in photonic quantum information applications. Besides being used in quantum computation, a cluster state also shows important applications in other fields such as quantum error correction, multipartite quantum communications and quantum metrology, as well as in the study of fundamental problems such as nonlocality and decoherence [198,199]. So far, with silicon photonic circuits, all types of four-photon graph states have been programmably generated [186], and a range of quantum information processing tasks with and without error-correction

encodings have been implemented, as shown in Fig. 8 [163]. The success rate was increased from 62.5% to 95.8% when running a phase-estimation algorithm using the error-correction program. Similar to MBQC, fusion-based quantum computation was proposed and developed in recent years by PsiQuantum [200,201]. With small-scale entangled photons as resource states and fusion-measurement, large-scale universal fault-tolerant quantum computing can be realized with on-chip components.

Other novel error-correction methods include entanglement purification and topologically electromagnetic modes. Entanglement purification is a way to extract a subset of states of high entanglement and high purity from a large set of less entangled states, which can significantly increase the quality of logic operations between different qubits and relax the requirement for high-accuracy logic operations [202]. The topologically electromagnetic modes are much less affected by nanophotonic fabrication-induced disorder and can be used to avoid errors. Up to now, topological quantum light sources [203–205] and quantum interference processes [206] on silicon photonic chips have been demonstrated.

C. Quantum Key Distribution

Governed by the laws of quantum mechanics, quantum key distribution (QKD) aims to share information with absolute security between the transmitters and receivers. After decades of development, QKD is becoming the building block of the quantum network, and many quantum encoding protocols have been developed, such as BB84, two-state, and the Einstein–Podolsky–Rosen protocol [2]. As a common information carrier choice, photons are distributed over a 803-km fiber [207], and from the satellite to the ground over a distance of up to 1200 km [10]. For convenience and practicality purposes, transmitters and receivers have been integrated on the photonic chip to achieve dense integration, high stability, and scalability [208], and are connected by single-mode or multicore fibers [187,209,210].

Through the combination of slow thermo-optic DC biases and a fast (10 GHz bandwidth) carrier-depletion modulation, high-speed low-error QKD modulation has been achieved with silicon photonic devices [209]. In addition, QKD systems with integrated silicon photonics have been demonstrated in an intercity metropolitan test with a 43-km fiber [211] and even full daylight [212]. The QKD system is becoming more compact and different degrees of freedom encoding have been implemented such as path [187], polarization [211], and time bins [95,213]. Based on hybrid techniques, photon lasers [214] and photon detection processes [79,95,96] have been integrated directly on the silicon chip. The high-dimensional QKD with quantum states generated in silicon photonic circuits allows the information efficiency limit of traditional quantum key distribution protocols to be surpassed [187]. With these technological advances, different key distribution protocols have been achieved with integrated silicon photonic devices such as BB84 [209], continuous-variable [215], and measurement-device-independent [216], as shown in Fig. 9.

D. Quantum State Teleportation

Quantum state teleportation aims to transfer a particle's quantum state to another particle rather than itself. As a new way of communications, this technique transfers quantum information carried in the quantum state with the help of quantum entanglement, and forms the basis of a scalable quantum network and distributed quantum computing. It involves three particles (A, B, C), and we assume particles B and C are Bell entangled. The quantum state of particle A can be transferred to particle B through Bell state measurement between A and C. With quantum state teleportation, a linear optical quantum information processor can be efficiently scaled by using a large number of cascaded gates [217]. The integrated quantum teleportation process was first implemented with silica slab waveguides [218], which was fabricated by the direct UV-writing technique. The silica waveguides have a large cross-section (typically 4.5 μm × 4.5 μm), and low chip-fiber coupling loss and transmission loss enable us to achieve single photons generated in free-space feeding into the chip directly through optical fibers while maintaining high brightness. In Ref. [218], four photons that were generated in free-space nonlinear crystals were used. Three photons were input into the chip, and the left one was input into the detector as heralding. On-chip interferometers were used to realize the functions of entanglement generation and Bell state measurement. Based on state measurement results, classical communications, and corresponding quantum state operations, the quantum state of one photon would be transferred to another photon.

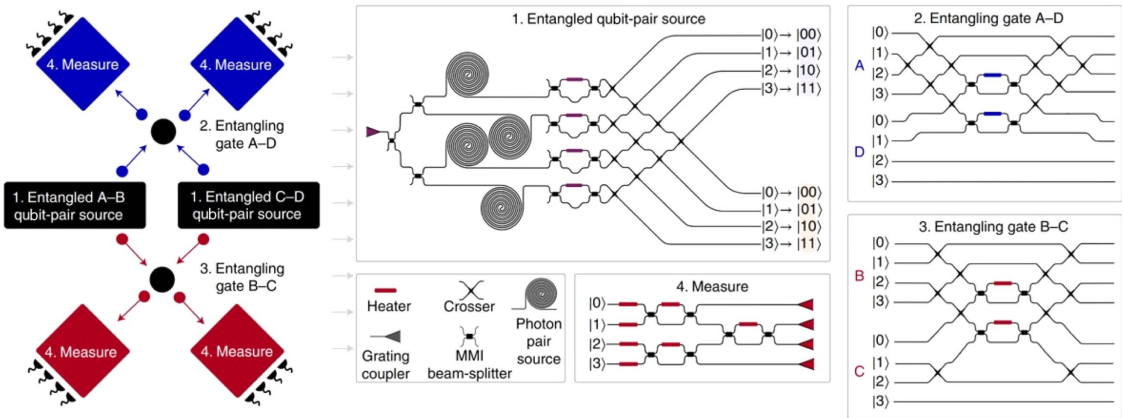

Fig. 8. Quantum error correction with silicon photonic devices. Error-protected qubits for quantum computation. Adapted from [163].

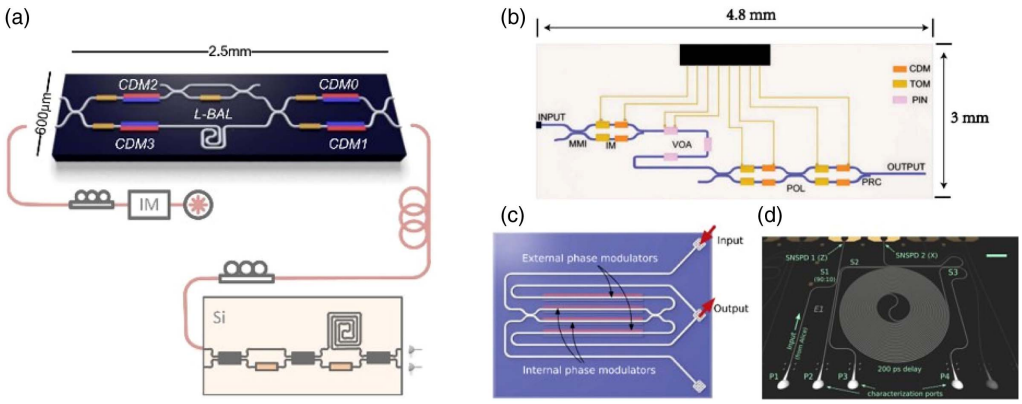

Fig. 9. Quantum key distribution (QKD) with silicon photonic devices. (a) Integrated devices for time-bin encoded BB84. Adapted from [209]. (b) Integrated devices for high-speed measurement-device-independent QKD. Adapted from [216]. (c) Silicon photonics encoder with high-speed electro-optic phase modulators. Adapted from [211]. (d) Detector-integrated on-chip QKD receiver. Adapted from [95].

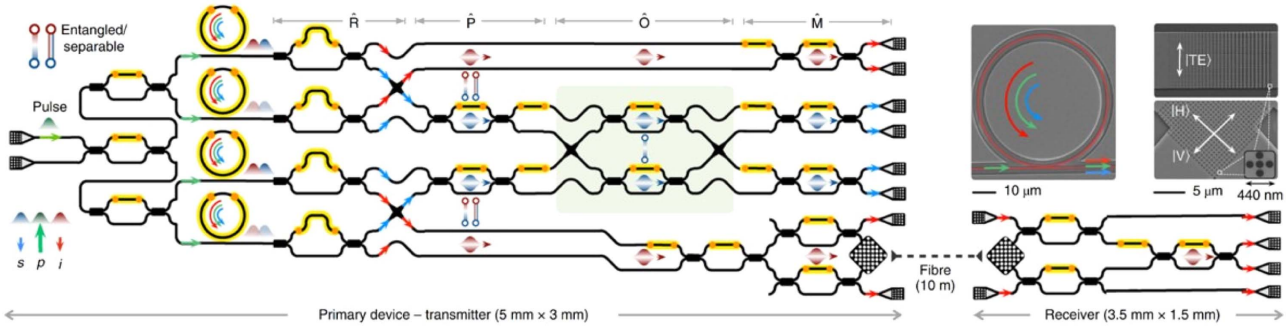

Fig. 10. Quantum state teleportation with silicon photonic devices. Chip-to-chip quantum teleportation. Adapted from [162].

Of course, quantum teleportation process can be achieved with silicon waveguides. In particular, strong SFWM in silicon waveguides can be used directly to manipulate multiphoton entangled quantum states. In Ref. [162], quantum teleportation between two silicon chips have been demonstrated, as shown in Fig. 10. Four microresonators were used to generate high-quality entangled quantum states directly on the silicon chip. Before the validation of the teleportation process, photons that obtained the quantum states were transmitted to another chip with a quantum photonic interconnect by path-polarization interconversion [219], where quantum states were reconstructed via state tomography measurements. This achievement lays the foundation for large-scale integrated photon quantum technology in communications and computing.

4. CHALLENGES AND OUTLOOK

Despite the progress mentioned above, further improvements are needed in some areas for scalable quantum information applications. Below, we outline some challenges in silicon photonic quantum technologies.

A. Low-Loss Components

Loss is a huge challenge for optical quantum integrated systems, including the loss of passive structures, delay lines, switches, and chip interconnects. Because of the small effective mode area, a loss in silicon is more prominent than in other materials, such as silica. Although a state-of-the-art low transmission loss of 0.08 dB/m has been demonstrated based on sidewall smoothing techniques [56], it is difficult to apply to waveguide structures with common strip waveguides. Multimode waveguide technology and mixing with silica or silicon nitride could enable the next generation of ultralow-loss components.

B. Photon Generation

For parametric photonic sources, the silicon waveguide has a strong two-photon absorption at 1550 nm, and it is difficult to enhance the brightness of the photonic sources just by increasing the pump power. In addition, the properties of the photonic sources are relatively poor, especially for multiphoton interference. A photonic source capable of large-scale expansion with high brightness is still on the way. Extending photons to the far infrared band, where silicon has low two-photon absorption, is one potential method. Another possible solution is to develop hybrid integrated silicon chips with other materials with better nonlinear properties, such as silicon nitride, in which the preparation of tens of photons has been demonstrated [220], and lithium niobate, which has a strong second-order nonlinear response. The stochastic character of the photon sources must be solved, and multiplexed photon sources,

long-time delay, and high-speed modulation should be integrated totally on the same chip. For deterministic single-photon sources, modulation to increase the indistinguishability between different sources should be developed.

C. Deterministic Quantum Operation

The negligible photon–photon interaction limits the applicability of many photon-based schemes. To overcome this limitation, multiplexed photon sources and feedforward capability based on heralded detection of auxiliary photons should be integrated totally on the same chip. Strong nonlinear media such as atoms must be introduced into the chip to enhance the photon–photon interaction to build deterministic multiphoton gates.

D. Frequency Conversion

Efficient frequency conversion will link various quantum systems to build up quantum networks, such as photonic conversion between a microwave wavelength and the telecom C-band. Efficient conversion at the single-photon level will allow us to take advantage of different systems, even if they are far away.

We have witnessed tremendous advances in silicon photonic devices for quantum information processing, especially in recent years. Photon sources as well as quantum state manipulation and detection can be integrated on a chip and hopefully on the same chip, and integrated programmable multiphoton and high-dimensional quantum information processors have been demonstrated. With further upgrading of fabrication technology, silicon photonics will have greater prospects in quantum information processing. Of course, silicon photonic devices still face many defects in the material itself, and the future quantum information processors are most likely to be hybrid with various materials elevated to the extreme. Despite challenges, we still believe that silicon photonics will play an important role.

Funding. National Natural Science Foundation of China (12004373, 61974168, 62005239, 62061160487, 62075243); Innovation Program for Quantum Science and Technology (2021ZD0303200); Natural Science Foundation of Zhejiang Province (LQ21F050006); National Key Research and Development Program of China (2017YFA0305200); Key Research and Development Program of Guangdong Province of China (2018B030325001, 2018B030329001); China Postdoctoral Science Foundation (2021T140647).

Disclosures. The authors declare no conflicts of interest.

Data Availability. Data underlying the results presented in this paper are not publicly available at this time but may be obtained from the authors upon reasonable request.

REFERENCES

1. C. H. Bennett and G. Brassard, "Quantum cryptography: public key distribution and coin tossing," in *Proceedings of the International Conference on Computers, Systems and Signal Processing* (1984), pp. 175–179.
2. N. Gisin, G. Ribordy, W. Tittel, and H. Zbinden, "Quantum cryptography," Rev. Mod. Phys. **74**, 145–195 (2002).
3. P. W. Shor, "Polynomial-time algorithms for prime factorization and discrete logarithms on a quantum computer," SIAM Rev. **41**, 303–332 (1999).
4. L. K. Grover, "Quantum mechanics helps in searching for a needle in a haystack," Phys. Rev. Lett. **79**, 325–328 (1997).
5. R. P. Feynman, "Simulating physics with computers," Int. J. Theor. Phys. **21**, 467–488 (1982).
6. V. Giovannetti, S. Lloyd, and L. Maccone, "Advances in quantum metrology," Nat. Photonics **5**, 222–229 (2011).
7. F. Arute, K. Arya, and R. Babbush et al., "Quantum supremacy using a programmable superconducting processor," Nature **574**, 505–510 (2019).
8. H.-S. Zhong, H. Wang, Y. H. Deng, M.-C. Chen, L.-C. Peng, Y.-H. Luo, J. Qin, D. Wu, X. Ding, Y. Hu, P. Hu, X.-Y. Yang, W.-J. Zhang, H. Li, Y. Li, X. Jiang, L. Gan, G. Yang, L. You, H. Wang, L. Li, N.-L. Liu, C.-Y. Lu, and J.-W. Pan, "Quantum computational advantage using photons," Science **370**, 1460–1463 (2020).
9. Y. Wu, W. S. Bao, S. Cao, F. Chen, M.-C. Chen, X. Chen, T.-H. Chung, H. Deng, Y. Du, D. Fan, M. Gong, C. Guo, C. Guo, S. Guo, L. Han, L. Hong, H.-L. Huang, Y.-H. Huo, L. Li, N. Li, S. Li, Y. Li, F. Liang, C. Lin, J. Lin, H. Qian, D. Qiao, H. Rong, H. Su, L. Sun, L. Wang, S. Wang, D. Wu, Y. Xu, K. Yan, W. Yang, Y. Yang, Y. Ye, J. Yin, C. Ying, J. Yu, C. Zha, C. Zhang, H. Zhang, K. Zhang, Y. Zhang, H. Zhao, Y. Zhao, L. Zhou, Q. Zhu, C.-Y. Lu, C.-Z. Peng, X. Zhu, and J.-W. Pan, "Strong quantum computational advantage using a superconducting quantum processor," Phys. Rev. Lett. **127**, 180501 (2021).
10. S. K. Liao, W. Q. Cai, W. Y. Liu, L. Zhang, Y. Li, J.-G. Ren, J. Yin, Q. Shen, Y. Cao, Z.-P. Li, F.-Z. Li, X.-W. Chen, L.-H. Sun, J.-J. Jia, J.-C. Wu, X.-J. Jiang, J.-F. Wang, Y.-M. Huang, Q. Wang, Y.-L. Zhou, L. Deng, T. Xi, L. Ma, T. Hu, Q. Zhang, Y.-A. Chen, N.-L. Liu, X.-B. Wang, Z.-C. Zhu, C.-Y. Lu, R. Shu, C.-Z. Peng, J.-Y. Wang, and J.-W. Pan, "Satellite-to-ground quantum key distribution," Nature **549**, 43–47 (2017).
11. B. P. Abbott, R. Abbott, and T. D. Abbott et al., "Observation of gravitational waves from a binary black hole merger," Phys. Rev. Lett. **116**, 061102 (2016).
12. J. M. Boss, K. S. Cujia, J. Zopes, and C. L. Degen, "Quantum sensing with arbitrary frequency resolution," Science **356**, 837–840 (2017).
13. Y. Zheng, L. M. Zhou, Y. Dong, C. W. Qiu, X. D. Chen, G. C. Guo, and F. W. Sun, "Robust optical-levitation-based metrology of nanoparticle's position and mass," Phys. Rev. Lett. **124**, 223603 (2020).
14. J. L. O'Brien, A. Furusawa, and J. Vučković, "Photonic quantum technologies," Nat. Photonics **3**, 687–695 (2009).
15. F. Flamini, N. Spagnolo, and F. Sciarrino, "Photonic quantum information processing: a review," Rep. Prog. Phys. **82**, 016001 (2018).
16. S. Slussarenko and G. J. Pryde, "Photonic quantum information processing: a concise review," Appl. Phys. Rev. **6**, 041303 (2019).
17. J. Wang, F. Sciarrino, A. Laing, and M. G. Thompson, "Integrated photonic quantum technologies," Nat. Photonics **14**, 273–284 (2020).
18. L. Lu, X. Zheng, Y. Lu, S. Zhu, and X. S. Ma, "Advances in chip-scale quantum photonic technologies," Adv. Quantum Technol. **4**, 2100068 (2021).
19. A. Politi, M. J. Cryan, J. G. Rarity, S. Yu, and J. L. O'Brien, "Silica-on-silicon waveguide quantum circuits," Science **320**, 646–649 (2008).
20. X. Jiang, L. Shao, S. X. Zhang, X. Yi, J. Wiersig, L. Wang, Q. Gong, M. Lončar, L. Yang, and Y. F. Xiao, "Chaos-assisted broadband momentum transformation in optical microresonators," Science **358**, 344–347 (2017).
21. X. Zhang, Q. T. Cao, Z. Wang, Y. X. Liu, C. W. Qiu, L. Yang, Q. Gong, and Y. F. Xiao, "Symmetry-breaking-induced nonlinear optics at a microcavity surface," Nat. Photonics **13**, 21–24 (2019).
22. M. Li, C. Li, Y. Chen, L. T. Feng, L. Yan, Q. Zhang, J. Bao, B. H. Liu, X. F. Ren, J. Wang, S. Wang, Y. Gao, X. Hu, Q. Gong, and Y. Li, "On-chip path encoded photonic quantum Toffoli gate," Photon. Res. **10**, 1533–1542 (2022).

23. J. W. Silverstone, D. Bonneau, J. L. O'Brien, and M. G. Thompson, "Silicon quantum photonics," IEEE J. Sel. Top. Quantum Electron. **22**, 390–402 (2016).
24. X. Zhang, B. A. Bell, A. Mahendra, C. Xiong, P. H. W. Leong, and B. J. Eggleton, "Integrated silicon nitride time-bin entanglement circuits," Opt. Lett. **43**, 3469–3472 (2018).
25. X. Lu, Q. Li, D. A. Westly, G. Moille, A. Singh, V. Anant, and K. Srinivasan, "Chip-integrated visible-telecom entangled photon pair source for quantum communication," Nat. Phys. **15**, 373–381 (2019).
26. C. Taballione, R. van der Meer, H. J. Snijders, P. Hooijschuur, J. P. Epping, M. de Goede, B. Kassenberg, P. Venderbosch, C. Toebes, H. van den Vlekkert, P. W. H. Pinkse, and J. J. Renema, "A universal fully reconfigurable 12-mode quantum photonic processor," Mater. Quantum. Technol. **1**, 035002 (2021).
27. S. Y. Ren, W. Yan, L. T. Feng, Y. Chen, Y. K. Wu, X. Z. Qi, X. J. Liu, Y. J. Cheng, B. Y. Xu, L. J. Deng, G. C. Guo, L. Bi, and X. F. Ren, "Single-photon nonreciprocity with an integrated magneto-optical isolator," Laser Photon. Rev. **16**, 2100595 (2022).
28. H. Jin, F. M. Liu, P. Xu, J. L. Xia, M. L. Zhong, Y. Yuan, J. W. Zhou, Y. X. Gong, W. Wang, and S. N. Zhu, "On-chip generation and manipulation of entangled photons based on reconfigurable lithium-niobate waveguide circuits," Phys. Rev. Lett. **113**, 103601 (2014).
29. C. Wang, X. Xiong, N. Andrade, V. Venkataraman, X. F. Ren, G. C. Guo, and M. Lončar, "Second harmonic generation in nano-structured thin-film lithium niobate waveguides," Opt. Express **25**, 6963–6973 (2017).
30. B. Y. Xu, L. Chen, J. Lin, L. T. Feng, R. Niu, Z. Y. Zhou, R. Gao, C. Dong, G. Guo, Q. Gong, Y. Cheng, Y. F. Xiao, and X. F. Ren, "Spectrally multiplexed and bright entangled photon pairs in a lithium niobate microresonator," Sci. China **65**, 294262 (2022).
31. R. J. Bojko, J. Li, L. He, T. Baehr-Jones, and M. Hochberg, "Electron beam lithography writing strategies for low loss, high confinement silicon optical waveguides," J. Vac. Sci. Technol. B **29**, 06F309 (2011).
32. K. Sugioka and Y. Cheng, "Ultrafast lasers-reliable tools for advanced materials processing," Light Sci. Appl. **3**, e149 (2014).
33. T. Rudolph, "Why I am optimistic about the silicon-photonic route to quantum computing," APL Photon. **2**, 030901 (2017).
34. D. Thomson, A. Zilkie, J. E. Bowers, T. Komljenovic, G. T. Reed, L. Vivien, D. Marris-Morini, E. Cassan, L. Virot, J. M. Fédéli, J. M. Hartmann, J. H. Schmid, D. X. Xu, F. Boeuf, P. O'Brien, G. Z. Mashanovich, and M. Nedeljkovic, "Roadmap on silicon photonics," J. Opt. **18**, 073003 (2016).
35. G. Son, S. Han, J. Park, K. Kwon, and K. Yu, "High-efficiency broadband light coupling between optical fibers and photonic integrated circuits," Nanophotonics **7**, 1845–1864 (2018).
36. N. C. Harris, D. Bunandar, M. Pant, G. R. Steinbrecher, J. Mower, M. Prabhu, T. Baehr-Jones, M. Hochberg, and D. Englund, "Large-scale quantum photonic circuits in silicon," Nanophotonics **5**, 456–468 (2016).
37. W. H. Pernice, C. Schuck, O. Minaeva, M. Li, G. N. Goltsman, A. V. Sergienko, and H. X. Tang, "High-speed and high-efficiency travelling wave single-photon detectors embedded in nanophotonic circuits," Nat. Commun. **3**, 1325 (2012).
38. L. T. Feng, G. C. Guo, and X. F. Ren, "Progress on integrated quantum photonic sources with silicon," Adv. Quantum Technol. **3**, 1900058 (2020).
39. X. Chen, Z. Fu, Q. Gong, and J. Wang, "Quantum entanglement on photonic chips: a review," Adv. Photon. **3**, 064002 (2021).
40. J. C. Adcock, J. Bao, Y. Chi, X. Chen, D. Bacco, Q. Gong, L. K. Oxenløwe, J. Wang, and Y. Ding, "Advances in silicon quantum photonics," IEEE J. Sel. Top. Quantum Electron. **27**, 6700224 (2020).
41. A. W. Elshaari, W. Pernice, K. Srinivasan, O. Benson, and V. Zwiller, "Hybrid integrated quantum photonic circuits," Nat. Photonics **14**, 285–298 (2020).
42. J. H. Kim, S. Aghaeimeibodi, J. Carolan, D. Englund, and E. Waks, "Hybrid integration methods for on-chip quantum photonics," Optica **7**, 291–308 (2020).
43. Y. H. Li, Z. Y. Zhou, L. T. Feng, W. T. Fang, S. L. Liu, S. K. Liu, K. Wang, X. F. Ren, D. S. Ding, L. X. Xu, and B. S. Shi, "On-chip multiplexed multiple entanglement sources in a single silicon nanowire," Phys. Rev. Appl. **7**, 064005 (2017).
44. C. Ma, X. Wang, V. Anant, A. D. Beyer, M. D. Shaw, and S. Mookherjea, "Silicon photonic entangled photon-pair and heralded single photon generation with CAR > 12,000 and $g^2(0) < 0.006$," Opt. Express **25**, 32995–33006 (2017).
45. Y. Liu, C. Wu, X. Gu, Y. Kong, X. Yu, R. Ge, X. Cai, X. Qiang, J. Wu, X. Yang, and P. Xu, "High-spectral-purity photon generation from a dual-interferometer-coupled silicon microring," Opt. Lett. **45**, 73–76 (2020).
46. B. M. Burridge, I. I. Faruque, J. G. Rarity, and J. Barreto, "High spectro-temporal purity single-photons from silicon micro-racetrack resonators using a dual-pulse configuration," Opt. Lett. **45**, 4048–4051 (2020).
47. S. Paesani, M. Borghi, S. Signorini, A. Maïnos, L. Pavesi, and A. Laing, "Near-ideal spontaneous photon sources in silicon quantum photonics," Nat. Commun. **11**, 2505 (2020).
48. Y. Zhou, Z. Wang, A. Rasmita, S. Kim, A. Berhane, Z. Bodrog, G. Adamo, A. Gali, I. Aharonovich, and W. B. Gao, "Room temperature solid-state quantum emitters in the telecom range," Sci. Adv. **4**, eaar3580 (2018).
49. H. Zhao, M. T. Pettes, Y. Zheng, and H. Htoon, "Site-controlled telecom-wavelength single-photon emitters in atomically-thin $MoTe_2$," Nat. Commun. **12**, 6753 (2021).
50. M. Hollenbach, Y. Berencén, U. Kentsch, M. Helm, and G. V. Astakhov, "Engineering telecom single-photon emitters in silicon for scalable quantum photonics," Opt. Express **28**, 26111–26121 (2020).
51. D. B. Higginbottom, A. T. K. Kurkjian, C. Chartrand, M. Kazemi, N. A. Brunelle, E. R. MacQuarrie, J. R. Klein, N. R. Lee-Hone, J. Stacho, M. Ruether, C. Bowness, L. Bergeron, A. DeAbreu, S. R. Harrigan, J. Kanaganayagam, D. W. Marsden, T. S. Richards, L. A. Stott, S. Roorda, K. J. Morse, M. L. W. Thewalt, and S. Simmons, "Optical observation of single spins in silicon," Nature **607**, 266–270 (2022).
52. M. J. Collins, C. Xiong, I. H. Rey, T. D. Vo, J. He, S. Shahnia, C. Reardon, T. F. Krauss, M. J. Steel, A. S. Clark, and B. J. Eggleton, "Integrated spatial multiplexing of heralded single-photon sources," Nat. Commun. **4**, 2582 (2013).
53. X. Zhang, I. Jizan, J. He, A. S. Clark, D.-Y. Choi, C. J. Chae, B. J. Eggleton, and C. Xiong, "Enhancing the heralded single-photon rate from a silicon nanowire by time and wavelength division multiplexing pump pulses," Opt. Lett. **40**, 2489–2492 (2015).
54. C. Xiong, X. Zhang, Z. Liu, M. J. Collins, A. Mahendra, L. G. Helt, M. J. Steel, D.-Y. Choi, C. J. Chae, P. H. W. Leong, and B. J. Eggleton, "Active temporal multiplexing of indistinguishable heralded single photons," Nat. Commun. **7**, 10853 (2016).
55. F. Kaneda and P. G. Kwiat, "High-efficiency single-photon generation via large-scale active time multiplexing," Sci. Adv. **5**, eaaw8586 (2019).
56. H. Lee, T. Chen, J. Li, O. Painter, and K. J. Vahala, "Ultra-low-loss optical delay line on a silicon chip," Nat. Commun. **3**, 867 (2012).
57. M. He, M. Xu, Y. Ren, J. Jian, Z. Ruan, Y. Xu, S. Gao, S. Sun, X. Wen, L. Zhou, L. Liu, C. Guo, H. Chen, S. Yu, L. Liu, and X. Cai, "High-performance hybrid silicon and lithium niobate Mach–Zehnder modulators for 100 Gbit s^{-1} and beyond," Nat. Photonics **13**, 359–364 (2019).
58. S. Haffouz, K. D. Zeuner, D. Dalacu, P. J. Poole, J. Lapointe, D. Poitras, K. Mnaymneh, X. Wu, M. Couillard, M. Korkusinski, E. Schöll, K. D. Jöns, V. Zwiller, and R. L. Williams, "Bright single InAsP quantum dots at telecom wavelengths in position-controlled InP nanowires: the role of the photonic waveguide," Nano Lett. **18**, 3047–3052 (2018).
59. J. H. Kim, S. Aghaeimeibodi, C. J. Richardson, R. P. Leavitt, D. Englund, and E. Waks, "Hybrid integration of solid-state quantum emitters on a silicon photonic chip," Nano Lett. **17**, 7394–7400 (2017).
60. T. Müller, J. Skiba-Szymanska, A. B. Krysa, J. Huwer, M. Felle, M. Anderson, R. M. Stevenson, J. Heffernan, D. A. Ritchie, and A. J. Shields, "A quantum light-emitting diode for the standard telecom window around 1,550 nm," Nat. Commun. **9**, 862 (2018).

61. R. Katsumi, Y. Ota, M. Kakuda, S. Iwamoto, and Y. Arakawa, "Transfer-printed single-photon sources coupled to wire waveguides," Optica **5**, 691–694 (2018).
62. R. Katsumi, Y. Ota, A. Osada, T. Yamaguchi, T. Tajiri, M. Kakuda, S. Iwamoto, H. Akiyama, and Y. Arakawa, "Quantum-dot single-photon source on a CMOS silicon photonic chip integrated using transfer printing," APL Photon. **4**, 036105 (2019).
63. W. Redjem, A. Durand, T. Herzig, A. Benali, S. Pezzagna, J. Meijer, A. Y. Kuznetsov, H. S. Nguyen, S. Cueff, J.-M. Gérard, I. Robert-Philip, B. Gil, D. Caliste, P. Pochet, M. Abbarchi, V. Jacques, A. Dréau, and G. Cassabois, "Single artificial atoms in silicon emitting at telecom wavelengths," Nat. Electron. **3**, 738–743 (2020).
64. M. Hollenbach, N. S. Jagtap, C. Fowley, J. Baratech, V. Guardia-Arce, U. Kentsch, A. Eichler-Volf, N. V. Abrosimov, A. Erbe, C. Shin, H. Kim, M. Helm, W. Lee, G. V. Astakhov, and Y. Berencén, "A photonic platform hosting telecom photon emitters in silicon," arXiv:2112.02680 (2021).
65. M. Prabhu, C. Errando-Herranz, L. D. Santis, I. Christen, C. Chen, and D. R. Englund, "Individually addressable artificial atoms in silicon photonics," arXiv:2202.02342 (2022).
66. L. Bergeron, C. Chartrand, A. T. K. Kurkjian, K. J. Morse, H. Riemann, N. V. Abrosimov, P. Becker, H. J. Pohl, M. L. W. Thewalt, and S. Simmons, "Silicon-integrated telecommunications photon-spin interface," PRX Quantum **1**, 020301 (2020).
67. S. Liu, K. Srinivasan, and J. Liu, "Nanoscale positioning approaches for integrating single solid-state quantum emitters with photonic nanostructures," Laser Photon. Rev. **15**, 2100223 (2021).
68. P. Peng, Y. C. Liu, D. Xu, Q. T. Cao, G. Lu, Q. Gong, and Y. F. Xiao, "Enhancing coherent light-matter interactions through microcavity-engineered plasmonic resonances," Phys. Rev. Lett. **119**, 233901 (2017).
69. S. Liu, Y. Wei, X. Li, Y. Yu, J. Liu, S. Yu, and X. Wang, "Dual-resonance enhanced quantum light-matter interactions in deterministically coupled quantum-dot-micropillars," Light Sci. Appl. **10**, 158 (2021).
70. Y. Wei, S. Liu, X. Li, Y. Yu, X. Su, S. Li, X. Shang, H. Liu, H. Hao, H. Ni, S. Yu, Z. Niu, J. Iles-Smith, J. Liu, and X. Wang, "Tailoring solid-state single-photon sources with stimulated emissions," Nat. Nanotechnol. **17**, 470–476 (2022).
71. R. B. Patel, A. J. Bennett, I. Farrer, C. A. Nicoll, D. A. Ritchie, and A. J. Shields, "Two-photon interference of the emission from electrically tunable remote quantum dots," Nat. Photonics **4**, 632–635 (2010).
72. E. B. Flagg, A. Muller, S. V. Polyakov, A. Ling, A. Migdall, and G. S. Solomon, "Interference of single photons from two separate semiconductor quantum dots," Phys. Rev. Lett. **104**, 137401 (2010).
73. A. W. Elshaari, E. Büyüközer, I. E. Zadeh, T. Lettner, P. Zhao, E. Schöll, S. Gyger, M. E. Reimer, D. Dalacu, P. J. Poole, K. D. Jöns, and V. Zwiller, "Strain-tunable quantum integrated photonics," Nano Lett. **18**, 7969–7976 (2018).
74. B. Machielse, S. Bogdanovic, S. Meesala, S. Gauthier, M. J. Burek, G. Joe, M. Chalupnik, Y. I. Sohn, J. Holzgrafe, R. E. Evans, C. Chia, H. Atikian, M. K. Bhaskar, D. D. Sukachev, L. Shao, S. Maity, M. D. Lukin, and M. Lončar, "Quantum interference of electromechanically stabilized emitters in nanophotonic devices," Phys. Rev. X **9**, 031022 (2019).
75. R. Katsumi, Y. Ota, A. Osada, T. Tajiri, T. Yamaguchi, M. Kakuda, S. Iwamoto, H. Akiyama, and Y. Arakawa, "*In situ* wavelength tuning of quantum-dot single-photon sources integrated on a CMOS-processed silicon waveguide," Appl. Phys. Lett. **116**, 041103 (2020).
76. L. Zhai, G. N. Nguyen, C. Spinnler, J. Ritzmann, M. C. Löbl, A. D. Wieck, A. Ludwig, A. Javadi, and R. J. Warburton, "Quantum interference of identical photons from remote GaAs quantum dots," Nat. Nanotechnol. **17**, 829–833 (2022).
77. N. H. Wan, T.-J. Lu, K. C. Chen, M. P. Walsh, M. E. Trusheim, L. D. Santis, E. A. Bersin, I. B. Harris, S. L. Mouradian, I. R. Christen, E. S. Bielejec, and D. Englund, "Large-scale integration of artificial atoms in hybrid photonic circuits," Nature **583**, 226–231 (2020).
78. D. Benedikovic, L. Virot, G. Aubin, F. Amar, B. Szelag, B. Karakus, J.-M. Hartmann, C. Alonso-Ramos, X. L. Roux, P. Crozat, E. Cassan, D. Marris-Morini, C. Baudot, F. Boeuf, J.-M. Fédéli, C. Kopp, and L. Vivien, "25 Gbps low-voltage hetero-structured silicon-germanium waveguide pin photodetectors for monolithic on-chip nanophotonic architectures," Photon. Res. **7**, 437–444 (2019).
79. F. Raffaelli, G. Ferranti, D. H. Mahler, P. Sibson, J. E. Kennard, A. Santamato, G. Sinclair, D. Bonneau, M. G. Thompson, and J. C. F. Matthews, "A homodyne detector integrated onto a photonic chip for measuring quantum states and generating random numbers," Quantum Sci. Technol. **3**, 025003 (2018).
80. J. F. Tasker, J. Frazer, G. Ferranti, E. J. Allen, L. F. Brunel, S. Tanzilli, V. D'Auria, and J. C. F. Matthews, "Silicon photonics interfaced with integrated electronics for 9 GHz measurement of squeezed light," Nat. Photonics **15**, 11–15 (2021).
81. C. Bruynsteen, M. Vanhoecke, J. Bauwelinck, and X. Yin, "Integrated balanced homodyne photonic-electronic detector for beyond 20 GHz shot-noise-limited measurements," Optica **8**, 1146–1152 (2021).
82. D. V. Reddy, R. R. Nerem, S. W. Nam, R. P. Mirin, and V. B. Verma, "Superconducting nanowire single-photon detectors with 98% system detection efficiency at 1550 nm," Optica **7**, 1649–1653 (2020).
83. B. Korzh, Q. Y. Zhao, J. P. Allmaras, S. Frasca, T. M. Autry, E. A. Bersin, A. D. Beyer, R. M. Briggs, B. Bumble, M. Colangelo, A. E. Dane, T. Gerrits, A. E. Lita, F. Marsili, G. Moody, C. Peña, E. Ramirez, J. D. Rezac, N. Sinclair, M. J. Stevens, A. E. Velasco, V. B. Verma, E. E. Wollman, S. Xie, D. Zhu, P. D. Hale, M. Spiropulu, K. L. Silverman, R. P. Mirin, S. W. Nam, A. G. Kozorezov, M. D. Shaw, and K. K. Berggren, "Demonstration of sub-3 ps temporal resolution with a superconducting nanowire single-photon detector," Nat. Photonics **14**, 250–255 (2020).
84. M. Akhlaghi, E. Schelew, and J. Young, "Waveguide integrated superconducting single-photon detectors implemented as near-perfect absorbers of coherent radiation," Nat. Commun. **6**, 8233 (2015).
85. J. Li, R. A. Kirkwood, L. J. Baker, D. Bosworth, K. Erotokritou, A. Banerjee, R. M. Heath, C. M. Natarajan, Z. H. Barber, M. Sorel, and R. H. Hadfield, "Nano-optical single-photon response mapping of waveguide integrated molybdenum silicide (MoSi) superconducting nanowires," Opt. Express **24**, 13931–13938 (2016).
86. S. Buckley, J. Chiles, A. N. McCaughan, G. Moody, K. L. Silverman, M. J. Stevens, R. P. Mirin, S. W. Nam, and J. M. Shainline, "All-silicon light-emitting diodes waveguide-integrated with superconducting single-photon detectors," Appl. Phys. Lett. **111**, 141101 (2017).
87. A. Vetter, S. Ferrari, P. Rath, R. Alaee, O. Kahl, V. Kovalyuk, S. Diewald, G. N. Goltsman, A. Korneev, C. Rockstuhl, and W. H. P. Pernice, "Cavity-enhanced and ultrafast superconducting single-photon detectors," Nano Lett. **16**, 7085–7092 (2016).
88. J. Münzberg, A. Vetter, F. Beutel, W. Hartmann, S. Ferrari, W. H. P. Pernice, and C. Rockstuhl, "Superconducting nanowire single-photon detector implemented in a 2D photonic crystal cavity," Optica **5**, 658–665 (2018).
89. D. Zhu, Q. Y. Zhao, H. Choi, T. J. Lu, A. E. Dane, D. Englund, and K. K. Berggren, "A scalable multi-photon coincidence detector based on superconducting nanowires," Nat. Nanotechnol. **13**, 596–601 (2018).
90. C. Cahall, K. L. Nicolich, N. T. Islam, G. P. Lafyatis, A. J. Miller, D. J. Gauthier, and J. Kim, "Multi-photon detection using a conventional superconducting nanowire single-photon detector," Optica **4**, 1534–1535 (2017).
91. D. Zhu, M. Colangelo, C. Chen, B. A. Korzh, F. N. C. Wong, M. D. Shaw, and K. K. Berggren, "Resolving photon numbers using a superconducting nanowire with impedance-matching taper," Nano Lett. **20**, 3858–3863 (2020).
92. Q. Y. Zhao, D. Zhu, N. Calandri, A. E. Dane, A. N. McCaughan, F. Bellei, H. Z. Wang, D. F. Santavicca, and K. K. Berggren, "Single-photon imager based on a superconducting nanowire delay line," Nat. Photonics **11**, 247–251 (2017).
93. E. E. Wollman, V. B. Verma, A. E. Lita, W. H. Farr, M. D. Shaw, R. P. Mirin, and S. W. Nam, "Kilopixel array of superconducting nanowire single-photon detectors," Opt. Express **27**, 35279–35289 (2019).

94. R. Cheng, C. L. Zou, X. Guo, S. Wang, X. Han, and H. X. Tang, "Broadband on-chip single-photon spectrometer," Nat. Commun. **10**, 4104 (2019).
95. F. Beutel, H. Gehring, M. A. Wolff, C. Schuck, and W. Pernice, "Detector-integrated on-chip QKD receiver for GHz clock rates," NPJ Quantum Inf. **7**, 40 (2021).
96. X. Zheng, P. Zhang, R. Ge, L. Lu, G. He, Q. Chen, F. Qu, L. Zhang, X. Cai, Y. Lu, S. N. Zhu, P. Wu, and X. Ma, "Heterogeneously integrated, superconducting silicon-photonic platform for measurement-device-independent quantum key distribution," Adv. Photon. **3**, 055002 (2021).
97. P. Vines, K. Kuzmenko, J. Kirdoda, D. C. S. Dumas, M. M. Mirza, R. W. Millar, D. J. Paul, and G. S. Buller, "High performance planar germanium-on-silicon single-photon avalanche diode detectors," Nat. Commun. **10**, 1086 (2019).
98. L. F. Llin, J. Kirdoda, F. Thorburn, L. L. Huddleston, Z. M. Greener, K. Kuzmenko, P. Vines, D. C. S. Dumas, R. W. Millar, G. S. Buller, and D. J. Paul, "High sensitivity Ge-on-Si single-photon avalanche diode detectors," Opt. Lett. **45**, 6406–6409 (2020).
99. J. Zhang, M. A. Itzler, H. Zbinden, and J. W. Pan, "Advances in InGaAs/InP single-photon detector systems for quantum communication," Light Sci. Appl. **4**, e286 (2015).
100. Y. Q. Fang, W. Chen, T. H. Ao, C. Liu, L. Wang, X. J. Gao, J. Zhang, and J. W. Pan, "InGaAs/InP single-photon detectors with 60% detection efficiency at 1550 nm," Rev. Sci. Instrum. **91**, 083102 (2020).
101. H. Wang, J. Guo, J. Miao, W. Luo, Y. Gu, R. Xie, F. Wang, L. Zhang, P. Wang, and W. Hu, "Emerging single-photon detectors based on low-dimensional materials," Small **18**, 2103963 (2022).
102. W. Song, R. Gatdula, S. Abbaslou, M. Lu, A. Stein, W. Y.-C. Lai, J. Provine, R. F. W. Pease, D. N. Christodoulides, and W. Jiang, "High-density waveguide superlattices with low crosstalk," Nat. Commun. **6**, 7027 (2015).
103. M. Zhang, L. T. Feng, M. Li, Y. Chen, L. Zhang, D. He, G. Guo, G. Guo, X. Ren, and D. Dai, "Supercompact photonic quantum logic gate on a silicon chip," Phys. Rev. Lett. **126**, 130501 (2021).
104. H. Zhou, Y. Wang, X. Gao, D. Gao, J. Dong, D. Huang, F. Li, P. A. Wai, and X. Zhang, "Dielectric metasurfaces enabled ultradensely integrated multidimensional optical system," Laser Photon. Rev. **16**, 2100521 (2022).
105. F. Horst, W. M. J. Green, S. Assefa, S. M. Shank, Y. A. Vlasov, and B. J. Offrein, "Cascaded Mach-Zehnder wavelength filters in silicon photonics for low loss and flat pass-band WDM (de-)multiplexing," Opt. Express **21**, 11652–11658 (2013).
106. S. Cheung, T. H. Su, K. Okamoto, and S. J. B. Yoo, "Ultra-compact silicon photonic 512×512 25 GHz arrayed waveguide grating router," IEEE J. Sel. Top. Quantum Electron. **20**, 310–316 (2014).
107. D. T. H. Tan, A. Grieco, and Y. Fainman, "Towards 100 channel dense wavelength division multiplexing with 100 GHz spacing on silicon," Opt. Express **22**, 10408–10415 (2014).
108. S. T. Chen, X. Fu, J. Wang, Y. C. Shi, S. L. He, and D. X. Dai, "Compact dense wavelength-division (de)multiplexer utilizing a bidirectional arrayed-waveguide grating integrated with a Mach–Zehnder interferometer," J. Lightwave Technol. **33**, 2279–2285 (2015).
109. D. Munk, M. Katzman, Y. Kaganovskii, N. Inbar, A. Misra, M. Hen, M. Priel, M. Feldberg, M. Tkachev, A. Bergman, M. Vofsi, M. Rosenbluh, T. Schneider, and A. Zadok, "Eight-channel silicon-photonic wavelength division multiplexer with 17 GHz spacing," IEEE J. Sel. Top. Quantum Electron. **25**, 8300310 (2019).
110. Z. Liu, J. Zhang, X. Li, L. Wang, J. Li, C. Xue, J. An, and B. Cheng, "25×50 Gbps wavelength division multiplexing silicon photonics receiver chip based on a silicon nanowire-arrayed waveguide grating," Photon. Res. **7**, 659–663 (2019).
111. J. R. Ong, R. Kumar, and S. Mookherjea, "Ultra-high-contrast and tunable-bandwidth filter using cascaded high-order silicon micro-ring filters," IEEE Photon. Technol. Lett. **25**, 1543–1546 (2013).
112. H. Qiu, J. Jiang, T. Hu, P. Yu, J. Yang, X. Jiang, and H. Yu, "Silicon add-drop filter based on multimode Bragg sidewall gratings and adiabatic couplers," J. Lightwave Technol. **35**, 1705–1709 (2017).
113. A. B. Price, P. Sibson, C. Erven, J. G. Rarity, and M. G. Thompson, "High-speed quantum key distribution with wavelength-division multiplexing on integrated photonic devices," in *Conference on Lasers and Electro-Optics* (2018), paper JTh2A.24.
114. D. Liu, H. Xu, Y. Tan, Y. Shi, and D. Dai, "Silicon photonic filters," Microw. Opt. Technol. Lett. **63**, 2252–2268 (2021).
115. S. Liao, Y. Ding, C. Peucheret, T. Yang, J. Dong, and X. Zhang, "Integrated programmable photonic filter on the silicon-on-insulator platform," Opt. Express **22**, 31993–31998 (2014).
116. F. Xia, M. Rooks, L. Sekaric, and Y. Vlasov, "Ultra-compact high order ring resonator filters using submicron silicon photonic wires for on-chip optical interconnects," Opt. Express **15**, 11934–11941 (2007).
117. P. Chen, S. Chen, X. Guan, Y. Shi, and D. Dai, "High-order microring resonators with bent couplers for a box-like filter response," Opt. Lett. **39**, 6304–6307 (2014).
118. D. Liu, C. Zhang, D. Liang, and D. Dai, "Submicron-resonator-based add-drop optical filter with an ultra-large free spectral range," Opt. Express **27**, 416–422 (2019).
119. N. C. Harris, D. Grassani, A. Simbula, M. Pant, M. Galli, T. Baehr-Jones, M. Hochberg, D. Englund, D. Bajoni, and C. Galland, "Integrated source of spectrally filtered correlated photons for large-scale quantum photonic systems," Phys. Rev. X **4**, 041047 (2014).
120. D. Oser, S. Tanzilli, F. Mazeas, C. Alonso-Ramos, X. L. Roux, G. Sauder, X. Hua, O. Alibart, L. Vivien, É. Cassan, and L. Labonté, "High-quality photonic entanglement out of a stand-alone silicon chip," NPJ Quantum Inf. **6**, 31 (2020).
121. C. Li, D. Liu, and D. Dai, "Multimode silicon photonics," Nanophotonics **8**, 227–247 (2019).
122. L. W. Luo, N. Ophir, C. P. Chen, L. H. Gabrielli, C. B. Poitras, K. Bergmen, and M. Lipson, "WDM-compatible mode-division multiplexing on a silicon chip," Nat. Commun. **5**, 3069 (2014).
123. D. Dai, J. Wang, S. Chen, S. Wang, and S. He, "Monolithically integrated 64-channel silicon hybrid demultiplexer enabling simultaneous wavelength- and mode-division-multiplexing," Laser Photon. Rev. **9**, 339–344 (2015).
124. S. Wang, X. Feng, S. Gao, Y. Shi, T. Dai, H. Yu, H.-K. Tsang, and D. Dai, "On-chip reconfigurable optical add-drop multiplexer for hybrid wavelength/mode-division-multiplexing systems," Opt. Lett. **42**, 2802–2805 (2017).
125. D. Guo and T. Chu, "Silicon mode (de)multiplexers with parameters optimized using shortcuts to adiabaticity," Opt. Express **25**, 9160–9170 (2017).
126. D. Dai, C. Li, S. Wang, H. Wu, Y. Shi, Z. Wu, S. Gao, T. Dai, H. Yu, and H. K. Tsang, "10-channel mode (de)multiplexer with dual polarizations," Laser Photon. Rev. **12**, 1700109 (2018).
127. H. Xu and Y. Shi, "Metamaterial-based Maxwell's fisheye lens for multimode waveguide crossing," Laser Photon. Rev. **12**, 1800094 (2018).
128. Y. Liu, K. Xu, S. Wang, W. Shen, H. Xie, Y. Wang, S. Xiao, Y. Yao, J. Du, Z. He, and Q. Song, "Arbitrarily routed mode-division multiplexed photonic circuits for dense integration," Nat. Commun. **10**, 3263 (2019).
129. Y. Xiong, R. Priti, and O. Ladouceur, "High-speed two-mode switch for mode-division multiplexing optical networks," Optica **4**, 1098–1102 (2017).
130. D. Dai, J. Wang, and Y. Shi, "Silicon mode (de)multiplexer enabling high capacity photonic networks-on-chip with a single-wavelength-carrier light," Opt. Lett. **38**, 1422–1424 (2013).
131. Y. Lai, Y. Yu, S. Fu, J. Xu, P. P. Shum, and X. Zhang, "Compact double-part grating coupler for higher-order mode coupling," Opt. Lett. **43**, 3172–3175 (2018).
132. S. Li, Y. Zhou, J. Dong, X. Zhang, E. Cassan, J. Hou, C. Yang, S. Chen, D. Gao, and H. Chen, "Universal multimode waveguide crossing based on transformation optics," Optica **5**, 1549–1556 (2018).
133. L. T. Feng, M. Zhang, Z. Y. Zhou, M. Li, X. Xiong, L. Yu, B. S. Shi, G. P. Guo, D. X. Dai, X. F. Ren, and G. C. Guo, "On-chip coherent conversion of photonic quantum entanglement between different degrees of freedom," Nat. Commun. **7**, 11985 (2016).

134. A. Mohanty, M. Zhang, A. Dutt, S. Ramelow, P. Nussenzveig, and M. Lipson, "Quantum interference between transverse spatial waveguide modes," Nat. Commun. **8**, 14010 (2017).
135. L. T. Feng, M. Zhang, X. Xiong, D. Liu, Y. J. Cheng, F. M. Jing, X. Z. Qi, Y. Chen, D. Y. He, G. P. Guo, G. C. Guo, D. X. Dai, and X. F. Ren, "Transverse mode-encoded quantum gate on a silicon photonic chip," Phys. Rev. Lett. **128**, 060501 (2022).
136. L. T. Feng, M. Zhang, X. Xiong, Y. Chen, H. Wu, M. Li, G. P. Guo, G. C. Guo, D. X. Dai, and X. F. Ren, "On-chip transverse-mode entangled photon pair source," NPJ Quantum Inf. **5**, 2 (2019).
137. J. Komma, C. Schwarz, G. Hofmann, D. Heinert, and R. Nawrodt, "Thermo-optic coefficient of silicon at 1550 nm and cryogenic temperatures," Appl. Phys. Lett. **101**, 041905 (2012).
138. M. Gehl, C. Long, D. Trotter, A. Starbuck, A. Pomerene, J. B. Wright, S. Melgaard, J. Siirola, A. L. Lentine, and C. DeRose, "Operation of high-speed silicon photonic micro-disk modulators at cryogenic temperatures," Optica **4**, 374–382 (2017).
139. F. Eltes, G. E. Villarreal-Garcia, D. Caimi, H. Siegwart, A. A. Gentile, A. Hart, P. Stark, G. D. Marshall, M. G. Thompson, J. Barreto, J. Fompeyrine, and S. Abel, "An integrated optical modulator operating at cryogenic temperatures," Nat. Mater. **19**, 1164–1168 (2020).
140. U. Chakraborty, J. Carolan, G. Clark, D. Bunandar, G. Gilbert, J. Notaros, M. R. Watts, and D. R. Englund, "Cryogenic operation of silicon photonic modulators based on the DC Kerr effect," Optica **7**, 1385–1390 (2020).
141. M. Dong, G. Clark, A. J. Leenheer, M. Zimmermann, D. Dominguez, A. J. Menssen, D. Heim, G. Gilbert, D. Englund, and M. Eichenfield, "High-speed programmable photonic circuits in a cryogenically compatible, visible-near-infrared 200 mm CMOS architecture," Nat. Photonics **16**, 59–65 (2022).
142. W. H. P. Pernice, C. Schuck, M. Li, and H. X. Tang, "Carrier and thermal dynamics of silicon photonic resonators at cryogenic temperatures," Opt. Express **19**, 3290–3296 (2011).
143. X. Sun, X. Zhang, C. Schuck, and H. X. Tang, "Nonlinear optical effects of ultrahigh-*Q* silicon photonic nanocavities immersed in superfluid helium," Sci. Rep. **3**, 1436 (2013).
144. G. F. Sinclair, N. A. Tyler, D. Sahin, J. Barreto, and M. G. Thompson, "Temperature dependence of the Kerr nonlinearity and two-photon absorption in a silicon waveguide at 1.55 μm," Phys. Rev. Appl. **11**, 044084 (2019).
145. D. Taillaert, W. Bogaerts, P. Bienstman, T. F. Krauss, P. Van Dale, I. Moerman, S. Verstuyft, K. De Mesel, and R. Baets, "An out-of-plane grating coupler for efficient butt-coupling between compact planar waveguides and single-mode fibers," IEEE J. Quantum Electron. **38**, 949–955 (2002).
146. F. V. Laere, T. Claes, J. Schrauwen, S. Scheerlinck, W. Bogaerts, D. Taillaert, L. O'Faolain, D. V. Thourhout, and R. Baets, "Compact focusing grating couplers for silicon-on-insulator integrated circuits," IEEE Photon. Technol. Lett. **19**, 1919–1921 (2007).
147. C. Li, H. Zhang, M. Yu, and G. Lo, "CMOS-compatible high efficiency double-etched apodized waveguide grating coupler," Opt. Express **21**, 7868–7874 (2013).
148. N. Hoppe, W. S. Zaoui, L. Rathgeber, Y. Wang, R. H. Klenk, W. Vogel, M. Kaschel, S. L. Portalupi, J. Burghartz, and M. Berroth, "Ultra-efficient silicon-on-insulator grating couplers with backside metal mirrors," IEEE J. Sel. Top. Quantum Electron. **26**, 8200206 (2020).
149. Q. Fang, J. Song, X. Luo, M. Yu, G. Lo, and Y. Liu, "Mode-size converter with high coupling efficiency and broad bandwidth," Opt. Express **19**, 21588–21594 (2011).
150. H. Luo, F. Xie, Y. Cao, S. Yu, L. Chen, and X. Cai, "Low-loss and broadband fiber-to-chip coupler by 3D fabrication on a silicon photonic platform," Opt. Lett. **45**, 1236–1239 (2020).
151. M. Trappen, M. Blaicher, P. I. Dietrich, C. Dankwart, Y. Xu, T. Hoose, M. R. Billah, A. Abbasi, R. Baets, U. Troppenz, M. Theurer, K. Wörhoff, M. Seyfried, W. Freude, and C. Koos, "3D-printed optical probes for wafer-level testing of photonic integrated circuits," Opt. Express **28**, 37996–38007 (2020).
152. N. Lindenmann, S. Dottermusch, M. L. Goedecke, T. Hoose, M. R. Billah, T. P. Onanuga, A. Hofmann, W. Freude, and C. Koos, "Connecting silicon photonic circuits to multicore fibers by photonic wire bonding," J. Lightwave Technol. **33**, 755–760 (2015).
153. P. I. Dietrich, M. Blaicher, I. Reuter, M. Billah, T. Hoose, A. Hofmann, C. Caer, R. Dangel, B. Offrein, U. Troppenz, M. Moehrle, W. Freude, and C. Koos, "*In situ* 3D nanoprinting of free-form coupling elements for hybrid photonic integration," Nat. Photonics **12**, 241–247 (2018).
154. Y. Tang, Z. Wang, L. Wosinski, U. Westergren, and S. He, "Highly efficient nonuniform grating coupler for silicon-on-insulator nanophotonic circuits," Opt. Lett. **35**, 1290–1292 (2010).
155. D. Benedikovic, P. Cheben, J. H. Schmid, D. X. Xu, J. Lapointe, S. Wang, R. Halir, A. Monux, S. Janz, and M. Dad, "High-efficiency single etch step apodized surface grating coupler using subwavelength structure," Laser Photon. Rev. **8**, L93–L97 (2014).
156. C. Li, K. S. Chee, J. Tao, H. Zhang, M. Yu, and G. Q. Lo, "Silicon photonics packaging with lateral fiber coupling to apodized grating coupler embedded circuit," Opt. Express **22**, 24235–24240 (2014).
157. R. Marchetti, C. Lacava, A. Khokhar, X. Chen, I. Cristiani, D. J. Richardson, G. T. Reed, P. Petropoulos, and P. Minzioni, "High-efficiency grating-couplers: demonstration of a new design strategy," Sci. Rep. **7**, 16670 (2017).
158. D. Vermeulen, S. Selvaraja, P. Verheyen, G. Lepage, W. Bogaerts, P. Absil, D. Van Thourhout, and G. Roelkens, "High-efficiency fiber-to-chip grating couplers realized using an advanced CMOS-compatible silicon-on-insulator platform," Opt. Express **18**, 18278–18283 (2010).
159. D. Taillaert, P. Bienstman, and R. Baets, "Compact efficient broadband grating coupler for silicon-on-insulator waveguides," Opt. Lett. **29**, 2749–2751 (2004).
160. Y. Ding, C. Peucheret, H. Ou, and K. Yvind, "Fully etched apodized grating coupler on the SOI platform with −0.58 dB coupling efficiency," Opt. Lett. **39**, 5348–5350 (2014).
161. S. Paesani, Y. Ding, R. Santagati, L. Chakhmakhchyan, C. Vigliar, K. Rottwitt, L. K. Oxenløwe, J. Wang, M. G. Thompson, and A. Laing, "Generation and sampling of quantum states of light in a silicon chip," Nat. Phys. **15**, 925–929 (2019).
162. D. Llewellyn, Y. Ding, and I. I. Faruque et al., "Chip-to-chip quantum teleportation and multi-photon entanglement in silicon," Nat. Phys. **16**, 148–153 (2020).
163. C. Vigliar, S. Paesani, Y. Ding, J. C. Adcock, J. Wang, S. Morley-Short, D. Bacco, L. K. Oxenløwe, M. G. Thompson, J. G. Rarity, and A. Laing, "Error-protected qubits in a silicon photonic chip," Nat. Phys. **17**, 1137–1143 (2021).
164. Y. Xue, H. Chen, Y. Bao, J. Dong, and X. Zhang, "Two-dimensional silicon photonic grating coupler with low polarization-dependent loss and high tolerance," Opt. Express **27**, 22268–22274 (2019).
165. M. Pu, L. Liu, H. Ou, K. Yvind, and J. M. Hvam, "Ultra-low-loss inverted taper coupler for silicon-on-insulator ridge waveguide," Opt. Commun. **283**, 3678–3682 (2010).
166. L. Jia, C. Li, T. Y. Liow, and G. Q. Lo, "Efficient suspended coupler with loss less than −1.4 dB between Si-photonic waveguide and cleaved single mode fiber," J. Lightwave Technol. **36**, 239–244 (2018).
167. N. Lindenmann, G. Balthasar, D. Hillerkuss, R. Schmogrow, M. Jordan, J. Leuthold, W. Freude, and C. Koos, "Photonic wire bonding: a novel concept for chip-scale interconnects," Opt. Express **20**, 17667–17677 (2012).
168. M. R. Billah, M. Blaicher, T. Hoose, P. I. Dietrich, P. Marin-Palomo, N. Lindenmann, A. Nesic, A. Hofmann, U. Troppenz, M. Moehrle, S. Randel, W. Freude, and C. Koos, "Hybrid integration of silicon photonics circuits and InP lasers by photonic wire bonding," Optica **5**, 876–883 (2018).
169. Y. Shen, N. C. Harris, S. Skirlo, M. Prabhu, T. Baehr-Jones, M. Hochberg, X. Sun, S. Zhao, H. Larochelle, D. Englund, and M. Soljačić, "Deep learning with coherent nanophotonic circuits," Nat. Photonics **11**, 441–446 (2017).
170. N. C. Harris, G. R. Steinbrecher, M. Prabhu, Y. Lahini, J. Mower, D. Bunandar, C. Chen, F. N. C. Wong, T. Baehr-Jones, M. Hochberg, S. Lloyd, and D. Englund, "Quantum transport simulations in a programmable nanophotonic processor," Nat. Photonics **11**, 447–452 (2017).

171. H. W. Rhee, J. Shim, J. Y. Kim, D. J. Bang, H. Yoon, M. Kim, C. C. Kim, J. B. You, and H. H. Park, "Direct optical wire bonding through open-to-air polymerization for silicon photonic chips," Opt. Lett. **47**, 714–717 (2022).
172. D. Istrati, Y. Pilnyak, J. C. Loredo, C. Antón, N. Somaschi, P. Hilaire, H. Ollivier, M. Esmann, L. Cohen, L. Vidro, C. Millet, A. Lemaître, I. Sagnes, A. Harouri, L. Lanco, P. Senellart, and H. S. Eisenberg, "Sequential generation of linear cluster states from a single photon emitter," Nat. Commun. **11**, 5501 (2020).
173. H. Wang, Y. He, Y. H. Li, Z. E. Su, B. Li, H. L. Huang, X. Ding, M. C. Chen, C. Liu, J. Qin, J. P. Li, Y. M. He, C. Schneider, M. Kamp, C. Z. Peng, S. Höfling, C. Y. Lu, and J. W. Pan, "High-efficiency multiphoton Boson sampling," Nat. Photonics **11**, 361–365 (2017).
174. H. Takesue, Y. Tokura, H. Fukuda, T. Tsuchizawa, T. Watanabe, K. Yamada, and S. Itabashi, "Entanglement generation using silicon wire waveguide," Appl. Phys. Lett. **91**, 201108 (2007).
175. H. Takesue, H. Fukuda, T. Tsuchizawa, T. Watanabe, K. Yamada, Y. Tokura, and S. Itabashi, "Generation of polarization entangled photon pairs using silicon wire waveguide," Opt. Express **16**, 5721–5727 (2008).
176. N. Matsuda, H. L. Jeannic, H. Fukuda, T. Tsuchizawa, W. J. Munro, K. Shimizu, K. Yamada, Y. Tokura, and H. Takesue, "A monolithically integrated polarization entangled photon pair source on a silicon chip," Sci. Rep. **2**, 817 (2012).
177. J. W. Silverstone, R. Santagati, D. Bonneau, M. J. Strain, M. Sorel, J. L. O'Brien, and M. G. Thompson, "Qubit entanglement between ring-resonator photon-pair sources on a silicon chip," Nat. Commun. **6**, 7948 (2015).
178. J. Wang, S. Paesani, R. Santagati, S. Knauer, A. A. Gentile, N. Wiebe, M. Petruzzella, J. L. O'Brien, J. G. Rarity, A. Laing, and M. G. Thompson, "Experimental quantum Hamiltonian learning," Nat. Phys. **13**, 551–555 (2017).
179. S. Paesani, A. A. Gentile, R. Santagati, J. Wang, N. Wiebe, D. P. Tew, J. L. O'Brien, and M. G. Thompson, "Experimental Bayesian quantum phase estimation on a silicon photonic chip," Phys. Rev. Lett. **118**, 100503 (2017).
180. X. Qiang, X. Zhou, J. Wang, C. M. Wilkes, T. Loke, S. O'Gara, L. Kling, G. D. Marshall, R. Santagati, T. C. Ralph, J. B. Wang, J. L. O'Brien, M. G. Thompson, and J. C. F. Matthews, "Large-scale silicon quantum photonics implementing arbitrary two-qubit processing," Nat. Photonics **12**, 534–539 (2018).
181. X. Qiang, Y. Wang, S. Xue, R. Ge, L. Chen, Y. Liu, A. Huang, X. Fu, P. Xu, T. Yi, F. Xu, M. Deng, J. B. Wang, J. D. A. Meinecke, J. C. F. Matthews, X. Cai, X. Yang, and J. Wu, "Implementing graph-theoretic quantum algorithms on a silicon photonic quantum walk processor," Sci. Adv. **7**, eabb8375 (2021).
182. K. Harada, H. Takesue, H. Fukuda, T. Tsuchizawa, T. Watanabe, K. Yamada, Y. Tokura, and S. Itabashi, "Indistinguishable photon pair generation using two independent silicon wire waveguides," New J. Phys. **13**, 065005 (2011).
183. I. I. Faruque, G. F. Sinclair, D. Bonneau, J. G. Rarity, and M. G. Thompson, "On-chip quantum interference with heralded photons from two independent micro-ring resonator sources in silicon photonics," Opt. Express **26**, 20379–20395 (2018).
184. M. Zhang, L. T. Feng, Z. Y. Zhou, Y. Chen, H. Wu, M. Li, S. M. Gao, G. P. Guo, G. C. Guo, D. X. Dai, and X. F. Ren, "Generation of multiphoton quantum states on silicon," Light Sci. Appl. **8**, 41 (2019).
185. L. T. Feng, M. Zhang, Z. Y. Zhou, Y. Chen, M. Li, D. X. Dai, H. L. Ren, G. P. Guo, G. C. Guo, M. Tame, and X. F. Ren, "Generation of a frequency-degenerate four-photon entangled state using a silicon nanowire," NPJ Quantum Inf. **5**, 90 (2019).
186. J. C. Adcock, C. Vigliar, R. Santagati, J. W. Silverstone, and M. G. Thompson, "Programmable four-photon graph states on a silicon chip," Nat. Commun. **10**, 3528 (2019).
187. Y. Ding, D. Bacco, K. Dalgaard, X. Cai, X. Zhou, K. Rottwitt, and L. K. Oxenløwe, "High-dimensional quantum key distribution based on multicore fiber using silicon photonic integrated circuits," NPJ Quantum Inf. **3**, 25 (2017).
188. J. Wang, S. Paesani, Y. Ding, R. Santagati, P. Skrzypczyk, A. Salavrakos, J. Tura, R. Augusiak, L. Mančinska, D. Bacco, D. Bonneau, J. W. Silverstone, Q. Gong, A. Acín, K. Rottwitt, L. K. Oxenløwe, J. L. O'Brien, A. Laing, and M. G. Thompson, "Multidimensional quantum entanglement with large-scale integrated optics," Science **360**, 285–291 (2018).
189. Y. Chi, J. Huang, and Z. Zhang et al., "A programmable qudit-based quantum processor," Nat. Commun. **13**, 1166 (2022).
190. L. T. Feng, M. Zhang, D. Liu, Y. J. Cheng, G. P. Guo, D. X. Dai, G. C. Guo, M. Krenn, and X. F. Ren, "Observation of nonlocal quantum interference between the origins of a four-photon state in a silicon chip," arXiv:2103.14277 (2021).
191. X. M. Hu, Y. Guo, B. H. Liu, Y. F. Huang, C. F. Li, and G. C. Guo, "Beating the channel capacity limit for superdense coding with entangled ququarts," Sci. Adv. **4**, eaat9304 (2018).
192. B. P. Lanyon, M. Barbieri, M. P. Almeida, T. Jennewein, T. C. Ralph, K. J. Resch, G. J. Pryde, J. L. O'Brien, A. Gilchrist, and A. G. White, "Simplifying quantum logic using higher-dimensional Hilbert spaces," Nat. Phys. **5**, 134–140 (2009).
193. L. Lu, L. Xia, Z. Chen, L. Chen, T. Yu, T. Tao, W. Ma, Y. Pan, X. Cai, Y. Lu, S. Zhu, and X. S. Ma, "Three-dimensional entanglement on a silicon chip," NPJ Quantum Inf. **6**, 30 (2020).
194. C. M. Wilkes, X. Qiang, J. Wang, R. Santagati, S. Paesani, X. Zhou, D. A. B. Miller, G. D. Marshall, M. G. Thompson, and J. L. O'Brien, "60 dB high-extinction auto-configured Mach–Zehnder interferometer," Opt. Lett. **41**, 5318–5321 (2016).
195. X. C. Yao, T. X. Wang, H. Z. Chen, W. B. Gao, A. G. Fowler, R. Raussendorf, Z. B. Chen, N. L. Liu, C. Y. Lu, Y. J. Deng, Y. A. Chen, and J. W. Pan, "Experimental demonstration of topological error correction," Nature **482**, 489–494 (2012).
196. M. V. Larsen, X. Guo, C. R. Breum, J. S. Neergaard-Nielsen, and U. L. Andersen, "Deterministic generation of a two-dimensional cluster state," Science **366**, 369–392 (2019).
197. W. Asavanant, Y. Shiozawa, S. Yokoyama, B. Charoensombutamon, H. Emura, R. N. Alexander, S. Takeda, J. Yoshikawa, N. C. Menicucci, H. Yonezawa, and A. Furusawa, "Generation of time-domain-multiplexed two-dimensional cluster state," Science **366**, 373–376 (2019).
198. M. Hein, W. Dür, J. Eisert, R. Raussendorf, M. Van den Nest, and H. J. Briegel, "Entanglement in graph states and its applications," arXiv:quant-ph/0602096 (2006).
199. N. Shettell and D. Markham, "Graph states as a resource for quantum metrology," Phys. Rev. Lett. **124**, 110502 (2020).
200. S. Bartolucci, P. Birchall, H. Bombin, H. Cable, C. Dawson, M. Gimeno-Segovia, E. Johnston, K. Kieling, N. Nickerson, M. Pant, F. Pastawski, T. Rudolph, and C. Sparrow, "Fusion-based quantum computation," arXiv:2101.09310 (2021).
201. H. Bombin, I. H. Kim, D. Litinski, N. Nickerson, M. Pant, F. Pastawski, S. Roberts, and T. Rudolph, "Interleaving: modular architectures for fault-tolerant photonic quantum computing," arXiv:2103.08612 (2021).
202. J. W. Pan, S. Gasparoni, R. Ursin, G. Weihs, and A. Zeilinger, "Experimental entanglement purification of arbitrary unknown states," Nature **423**, 417–422 (2003).
203. S. Mittal, E. A. Goldschmidt, and M. Hafezi, "A topological source of quantum light," Nature **561**, 502–506 (2018).
204. M. Wang, C. Doyle, B. Bell, M. J. Collins, E. Magi, B. J. Eggleton, M. Segev, and A. Blanco-Redondo, "Topologically protected entangled photonic states," Nanophotonics **8**, 1327–1335 (2019).
205. T. Dai, Y. Ao, J. Bao, J. Mao, Y. Chi, Z. Fu, Y. You, X. Chen, C. Zhai, B. Tang, Y. Yang, Z. Li, L. Yuan, F. Gao, X. Lin, M. G. Thompson, J. L. O'Brien, Y. Li, X. Hu, Q. Gong, and J. Wang, "Topologically protected quantum entanglement emitters," Nat. Photonics **16**, 248–257 (2022).
206. Y. Chen, X. T. He, Y. J. Cheng, H. Y. Qiu, L. T. Feng, M. Zhang, D. X. Dai, G. C. Guo, J. W. Dong, and X. F. Ren, "Topologically protected valley-dependent quantum photonic circuits," Phys. Rev. Lett. **126**, 230503 (2021).
207. S. Wang, Z. Q. Yin, D. Y. He, W. Chen, R. Q. Wang, P. Ye, Y. Zhou, G. J. Fan-Yuan, F. X. Wang, W. Chen, Y. G. Zhu, P. V. Morozov, A. V. Divochiy, Z. Zhou, G. C. Guo, and Z. F. Han, "Twin-field quantum key distribution over 830-km fibre," Nat. Photonics **16**, 154–161 (2022).

208. Q. Wang, Y. Zheng, C. Zhai, X. Li, Q. Gong, and J. Wang, "Chip-based quantum communications," J. Semicond. **42**, 091901 (2021).
209. P. Sibson, J. E. Kennard, S. Stanisic, C. Erven, J. L. O'Brien, and M. G. Thompson, "Integrated silicon photonics for high-speed quantum key distribution," Optica **4**, 172–177 (2017).
210. D. Bacco, Y. Ding, K. Dalgaard, K. Rottwitt, and L. K. Oxenløwe, "Space division multiplexing chip-to-chip quantum key distribution," Sci. Rep. **7**, 12459 (2017).
211. D. Bunandar, A. Lentine, C. Lee, H. Cai, C. M. Long, N. Boynton, N. Martinez, C. DeRose, C. Chen, M. Grein, D. Trotter, A. Starbuck, A. Pomerene, S. Hamilton, F. N. C. Wong, R. Camacho, P. Davids, J. Urayama, and D. Englund, "Metropolitan quantum key distribution with silicon photonics," Phys. Rev. X **8**, 021009 (2018).
212. M. Avesani, L. Calderaro, M. Schiavon, A. Stanco, C. Agnesi, A. Santamato, M. Zahidy, A. Scriminich, G. Foletto, G. Contestabile, M. Chiesa, D. Rotta, M. Artiglia, A. Montanaro, M. Romagnoli, V. Sorianello, F. Vedovato, G. Vallone, and P. Villoresi, "Full daylight quantum-key-distribution at 1550 nm enabled by integrated silicon photonics," NPJ Quantum Inf. **7**, 93 (2019).
213. W. Geng, C. Zhang, Y. Zheng, J. He, C. Zhou, and Y. Kong, "Stable quantum key distribution using a silicon photonic transceiver," Opt. Express **27**, 29045–29054 (2019).
214. C. Agnesi, B. Da Lio, D. Cozzolino, L. Cardi, B. Ben Bakir, K. Hassan, A. Della Frera, A. Ruggeri, A. Giudice, G. Vallone, P. Villoresi, A. Tosi, K. Rottwitt, Y. Ding, and D. Bacco, "Hong–Ou–Mandel interference between independent III–V on silicon waveguide integrated lasers," Opt. Lett. **44**, 271–274 (2019).
215. G. Zhang, J. Y. Haw, H. Cai, F. Xu, S. M. Assad, J. F. Fitzsimons, X. Zhou, Y. Zhang, S. Yu, J. Wu, W. Ser, L. C. Kwek, and A. Q. Liu, "An integrated silicon photonic chip platform for continuous-variable quantum key distribution," Nat. Photonics **13**, 839–842 (2019).
216. K. Wei, W. Li, H. Tan, Y. Li, H. Min, W. J. Zhang, H. Li, L. You, Z. Wang, X. Jiang, T. Y. Chen, S. K. Liao, C. Z. Peng, F. Xu, and J. W. Pan, "High-speed measurement-device-independent quantum key distribution with integrated silicon photonics," Phys. Rev. X **10**, 031030 (2020).
217. P. Kok, K. Nemoto, T. C. Ralph, J. P. Dowling, and G. J. Milburn, "Linear optical quantum computing with photonic qubits," Rev. Mod. Phys. **79**, 135–174 (2007).
218. B. J. Metcalf, J. B. Spring, P. C. Humphreys, N. Thomas-Peter, M. Barbieri, W. S. Kolthammer, X. M. Jin, N. K. Langford, D. Kundys, J. C. Gates, B. J. Smith, P. G. R. Smith, and I. A. Walmsley, "Quantum teleportation on a photonic chip," Nat. Photonics **8**, 770–774 (2014).
219. J. Wang, D. Bonneau, M. Villa, J. W. Silverstone, R. Santagati, S. Miki, T. Yamashita, M. Fujiwara, M. Sasaki, H. Terai, M. G. Tanner, C. M. Natarajan, R. H. Hadfield, J. L. O'Brien, and M. G. Thompson, "Chip-to-chip quantum photonic interconnect by path-polarization interconversion," Optica **3**, 407–413 (2016).
220. J. M. Arrazola, V. Bergholm, and K. Brádler et al., "Quantum circuits with many photons on a programmable nanophotonic chip," Nature **591**, 54–60 (2021).